ORIGINAL RESEARCH PAPER

GENERAL MEDICINE

STRUCTURAL, TOPOLOGICAL, ELECTRONIC AND VIBRATIONAL PROPERTIES OF THE ANTIVIRAL TRIFLURIDINE AGENT. THEIR COMPARISON WITH THYMIDINE

KEY WORDS: Trifluridine, molecular structure, vibrational spectra, force field, DFT calculations

Silvia Antonia Brandán

Cátedra de Química General, Instituto de Química Inorgánica, Facultad de Bioquímica, Química y Farmacia, Universidad Nacional de Tucumán, Ayacucho 471,(4000), San Miguel de Tucumán, Tucumán, R, Argentina

ABSTRACT

The molecular structures of five stable isomers of trifluridine (TFT) have been studied by using the hybrid B3LYP/6-31G* method in gas and aqueous solution phases. The most stable structures are in very good agreement with that experimental determined by X-ray diffraction. The results show that both Cis conformations are the most stable than the other ones while the presence of the F atoms in the structure of TFT increase the volume, as compared with thymidine. The charges on the C atoms attached to the F atoms in TFT are higher and positive in relation to thymidine. The natural bond orbital (NBO) calculations reveal a higher stability for thymidine than TFT while the quantum atoms in molecules (QAIM) studies support the high stabilities of the Cis isomers in both antiviral agents. The frontier orbitals show that the CF_3 groups in the pyrimidine rings increase the gap values diminishing their reactivities while the descriptors demonstrate that the incorporation of CF_3 groups in the pyrimidine rings increases the electrophilicity and nucleophilicity indexes in TFT, as compared with thymidine. The complete assignments of the isomers of TFT, the force fields and the force constants are presented for the three isomers of TFT..

INTRODUCTION

The presence of chiral centres in the structures of antiviral nucleoside agents such as, emtricitabine, idoxuridine or trifluorothymidine (TFT) together with the existence of different groups in the pyrimidine rings evidently can explains their biological activities and their different structural and vibrational properties [1-4]. Thus, in these antiviral agents theoretically four isomers are expected as a consequence of the two asymmetric C atoms in the sugar ring [4] and, besides, other additional conformers can be present due to the different positions of the C-C-C-O side chain belonging to the ribose rings. In many cases, the combination of these agents with other substances produce a better therapeutic effect [5], as recently was reported by Nukatsuka et al. [6] for the mixed of TAS-102 and Oxaliplatin used in the treatment of human colorectal and gastric cancer xenografts. Thus, this TAS-102 substance is a mixed of trifluridine and tipiracil hydrochloride, a thymidine phosphorylase inhibitor, as mentioned by Tanaka et al. [7]. In other study, Azijli et al. [8] have showed the benefit of use TRAIL, a tumor selective anticancer agent, with a thymidylate synthase inhibitor for the treatment of non-small cell lung cancer. On the other hand, Bijnsdorp et al. have related the trifluorothymidine resistance to thymidine kinase, nucleoside transporter expression or phospholipase A2 [9] while Langen and Kowolljk [10] have determined that 5'-deoxy-5'-fluoro-thymidine inhibit the DNA synthesis. This way, taking into account the antiviral property [1,2] and the strong antitumor activity that present trifluridine or trifluorothymidine [6-11], an industrial enzymatic synthesis with high conversion of trifluridine was obtained from Psychrophilic Bacterium *Bacillus psychrosaccharolyticus* by Fresco-Taboada et al. [12]. The crystal and molecular structure of trifluridine or, also named 5-trifluoromethyl-2'-deoxyuridine was determined by Low et al. [13]. In that study the molecular packing of trifluridine shows small N---O, O---O and F---F contacts between different molecules. For this reason, the study of dimeric species of TFT is of interest to explain the variations in their properties in relation to other antiviral agents with similar structures. On the other hand, the presence of a CF_3 group in TFT and of those contacts in the experimental structure could explain their properties, as observed in similar nucleosides [14-16]. In this work, the structural, topological, electronic and vibrational properties of five stable isomers of trifluridine were studied in order to explain the differences that exist with thymidine due to the presence in the pyrimidine ring of the CF_3 group. Thus, DFT calculations in gas and aqueous solution phases by using the hybrid B3LYP method and the 6-31G* basis set [17,18] were performed. The SCRF methodology and the PCM model [19,20] were employed to calculate the properties in solution while the solvation model was used to compute the solvation energies [21]. The hydration volume was also calculated for explain the variations observed in the dipole moment values of those species in solution [22]. The optimized geometries were used to calculate the harmonic frequencies and the corresponding force fields at the same level of theory. In this case, the SQMFF methodology and the normal internal coordinates together with the Molvib program [23,24] were used to perform the vibrational assignments of the most stable isomers in both phases. The experimental and theoretical ^{1}H-NMR, ^{13}C-NMR and UV-visible spectra of TFT were compared with those corresponding to thymidine evidencing clearly the differences between both species. Here, the shifting toward high fields of the H atoms belonging to the CH and NH group of the pyrimidine ring of TFT is very evident as a consequence of the CF_3 group. In addition, it is remarkable as the three F atoms shift the signal of the C20 atoms toward high fields. The energy gap and of some useful descriptors calculations by means the frontier orbitals have revealed that the presence of the CF_3 group in TFT decrease the reactivity values in both media according increase the electrophilicity indexes, as compared with thymidine.

COMPUTATIONAL DETAILS

Initially, five isomers of TFT have been considered due to the presence of the two chiral C11 and C14 atoms. These structures were modeled with the *GaussView* program [25] and, later, they were optimized in gas and aqueous solution using the B3LYP/6-31G* method with the Gaussian program [26]. The structures of those five isomers of TFT named C1, C2, C3, C4 and C5 can be seen in **Figure 1.**

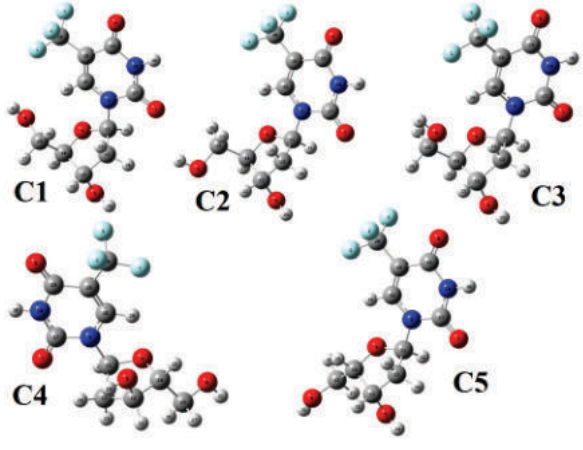

Figure 1. Theoretical structures and atoms numbering for the stable C1, C2, C3, C4 and C5 isomers of trifluoridine

The optimized Cartesian coordinates for the most stable C1, C3 and C5 structures were employed to compute their atomic

charges, molecular electrostatic potential, bond orders, delocalization energy, solvation energy and topological properties by using the NBO and QAIM calculations at the same level of theory [27,28]. The harmonic frequencies were also calculated in order to check the stationary points. The frontier orbitals and some descriptors were also computed using the same level approximation in order to predict behaviour and reactivities in the two media [29-36]. The force fields in both media were calculated using the SQMFF procedure and the internal coordinates with the Molvib program [23,24]. The contraction or expansion volumes that experiment those species in solution were calculated with the Moldraw program [22]. The prediction of the ^{1}H-NMR and ^{13}C-NMR spectra in aqueous solution were carry out with the GIAO method [37] while the time dependent density functional theory (TD-DFT) calculations were used to predict the ultraviolet-visible spectra of those most stable isomers in solution at B3LYP/6-31G* level of theory.

RESULTS AND DISCUSSION

Optimized geometries

Total and relative energies, dipole moment values and populations in both media for the five stable isomers of TFT are summarized in Table 1.

TABLE – 1 Total (E) and relative (ΔE) energies and dipole moment (μ) for all conformers of trifluridine

B3LYP/6-31G*				
Conf.	E (Hartree)	ΔE (kJ/mol)	μ (D)	Population analysis (%)
Gas phase[a]				
C1	-1172.8357	14.95	6.53	0.24
C2	-1172.8360	14.16	5.60	0.32
C3	-1172.8414	0.00	6.80	98.84
C4	-1172.8353	16.00	8.38	0.16
C5	-1172.8363	13.38	6.67	0.44
Aqueous solution[a]				
C1	-1172.8709	1.57	9.04	22.19
C2	-1172.8691	6.29	7.33	3.30
C3	-1172.8715	0.00	8.88	41.84
C4	-1172.8687	7.34	7.98	2.13
C5	-1172.8712	0.79	11.61	30.54

The population analysis shows that C3 is the isomer most stable in gas phase while probably C1, C3 and C5 are present in solution because they have approximately similar values, having slightly higher value C3. C1 and C3 are *Cis* isomers while C5 has *Trans* configuration. Note that these three isomers have the higher dipole moment values in solution as a consequence of their hydrations with water molecules. **Figure 2** shows the behaviours of the dipole moment values with the different isomers in solution where we can clearly see that C5 exhibit the higher value in solution.

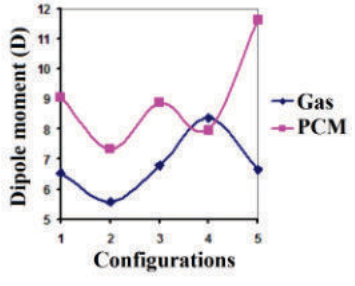

Figure 2. Variations of the dipole moment values corresponding to the most stable isomers of trifluridine in function of the different configurations in gas and aqueous solution phases at B3LYP/6-31G* level of theory.

Comparing the dipole moment values in solution for the most stable C3 conformers of thymidine (11.06 D) and TFT (8.88 D), we observed that the effect of the CF3 group in TFT is justly the decreasing of that value and the change in their direction, as observed in **Figure 3**.

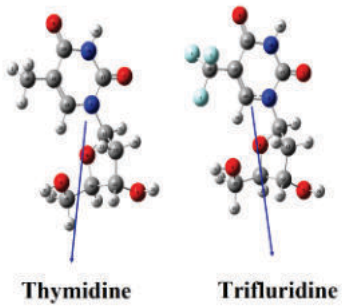

Figure 3. Comparisons between the magnitude and directions of the dipole moment values of the most stable isomers of thymidine and trifluridine in gas phase at B3LYP/6-31G* level of theory.

Analyzing the different volume variations that experiment the five isomers in solution, whose results are presented in **Table 2**, it is observed that the most stable isomer in solution, C3, has the lower volume variation while C5 undergo volume contraction in solution and, only C1 present expansion in this medium due probably to their low population in solution, in relation to C3 and C5. The behaviours of the volumes in both media are clearly represented in **Figure 4**.

TABLE – 2 Molecular volume for the stable conformations of Trifluridine by the B3LYP/6-31G* method

Trifluridine			
	Molar Volume (Å^3)		#V= V_{AS} – V_G (Å^3)
Conf.	GAS	PCM/SMD	
C1	255.5	256.8	1.3
C2	260.1	276.7	16.3
C3	254.6	254.2	-0.4
C4	264.5	266.6	2.1
C5	258.5	256.5	-2.0

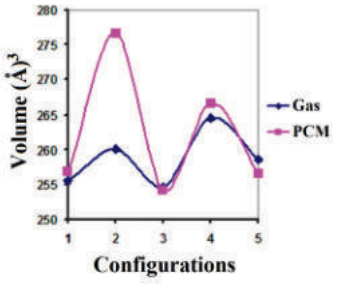

Figure 4. Volume variations of the most stable isomers of trifluridine in function of the configurations in gas and aqueous solution phases at B3LYP/6-31G* level of theory.

A comparison of the calculated geometrical parameters for the most stable isomers of TFT in gas and aqueous solution phases, according to the energetical stability of Table 1, with the corresponding experimental ones [13] can be seen in **Table 3** together with the root-mean-square deviation (RMSD) values. The calculated bond lengths and angles in both media show a very good correlation, presenting the C1, C3 and C5 isomers RMSD values between 0.024 and 0.022 Å for the bond lengths and between 2.6 and 2.0ş for the bond angles, respectively. Note that in general the B3LYP/6-31G* calculations predicted geometrical parameters higher than the experimental ones and that C3 present the better correlation in the bond angles. On the other hand, the O4-C11-N9-C17 and O4-C11-N9-C16 dihedral angles evidence that both isomers, C3 in gas phase and C5 in solution, have the better correlations with the experimental structure [13]. The scheme of H bond experimentally observed in thymidine is similar

to that observed in TFT, for this reason, the dimeric species of TFT was also studied. **Figure 5** shows the dimeric species of the C3 isomer of TFT in gas phase at B3LYP/6-31G* level of calculation.

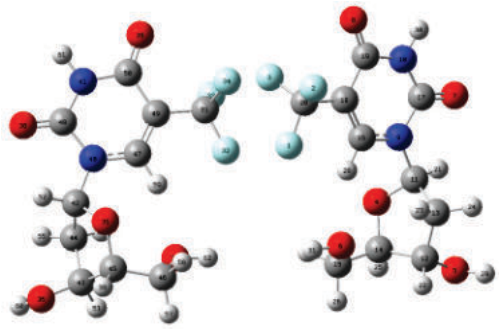

Figure 5. Dimeric species of trifluridine in gas phase at B3LYP/6-31G* level of calculation. Intramolecular H-bonds are represented with dashed lines.

The distances calculated between the more electronegative atoms for the stable conformations of TFT can be seen in **Table 4**. In general, the highest F-O and O-O distances are observed in the C3 isomer in both media while in relation to the N-O distances, C1 present the higher values in both media.

TABLE – 3 Comparison of calculated geometrical parameters for the most stable isomers of trifluridine in gas and aqueous solution phases

B3LYP/6-31G*[a]						
Parameters	C1	C3		C5		Exp[b]
	PCM	Gas phase	PCM	Gas phase	PCM	
Bond lengths (Å)						
C18-C20	1.492	1.497	1.492	1.498	1.492	1.504(16
C16-C18	1.360	1.354	1.357	1.356	1.358	1.348(14)
C18-C19	1.449	1.462	1.451	1.461	1.451	1.438(14)
C17-O7	1.227	1.218	1.226	1.220	1.226	1.177(12)
C17-N9	1.392	1.405	1.397	1.400	1.395	1.379(12)
C19-N10	1.395	1.409	1.394	1.411	1.394	1.380(18)
C16-N9	1.359	1.369	1.366	1.365	1.362	1.382(12)
C17-N10	1.379	1.383	1.380	1.381	1.380	1.414(13)
C19-O8	1.232	1.217	1.231	1.217	1.231	1.223(13)
N9-C11	1.501	1.473	1.481	1.490	1.490	1.490(11)
C11-O4	1.409	1.419	1.421	1.410	1.417	1.403(12)
C11-C13	1.537	1.535	1.532	1.538	1.536	1.529(12)
C12-C13	1.535	1.531	1.530	1.533	1.531	1.518(13)
C14-C12	1.528	1.541	1.536	1.532	1.531	1.496(14)
RMSD	**0.022**	**0.024**	**0.022**	**0.022**	**0.022**	
Bond angles (°)						
N10-C19-O8	120.5	120.6	120.6	120.5	120.6	119.9(12)
N10-C17-O7	122.8	123.1	122.1	123.7	122.4	121.1(11)
C19-C18-C20	118.8	118.9	118.7	118.8	118.6	120.8(12)
C16-C18-C20	121.1	121.0	121.2	121.0	121.4	119.1(12)
C17-N9-C16	121.6	121.8	121.5	121.8	121.5	123.0(10)
N9-C11-O4	108.9	108.3	108.1	109.0	108.8	108.3(8)
N9-C11-C13	112.9	114.1	114.3	113.2	113.3	111.9(9)
C11-O4-C14	110.7	111.1	110.9	110.3	109.9	107.3(9)
C13-C11-O4	107.3	106.0	106.6	106.6	106.8	105.1(8)
C11-C13-C12	103.1	102.5	102.6	101.8	102.4	99.6(8)
C12-C14-O4	104.5	106.3	105.7	105.0	104.8	107.6(9)
C14-C15-O6	108.2	109.1	110.6	106.0	107.0	112.1(14)
RMSD	**2.4**	**2.1**	**2.0**	**2.6**	**2.4**	
Dihedral angle (°)						
O4-C11-N9-C17	-163.1	-130.1	-124.0	-167.1	-144.2	-143.0
O4-C11-N9-C16	18.5	47.5	51.7	11.5	38.8	47.5
C13-C11-N9-C17	77.7	111.9	117.3	74.1	97.0	
C13-C11-N9-C16	-100.6	-70.3	-66.8	-107.0	-79.8	
N9-C16-C18-C20	-179.5	-179.7	-179.6	-179.8	179.8	
O4-C14-C15-O6	54.0	-68.3	-69.8	-170.8	-175.4	
O4-C14-C12-O5	-84.4	-93.9	-91.7	-81.9	-81.5	
N9-C11-O4-C14	-120.5	-138.6	-135.6	-128.4	-125.6	
N9-C11-C13-C12	139.4	149.6	147.7	147.8	145.5	
RMSD	**25.0**	**9.1**	**13.8**	**30.6**	**6.2**	

[a]This work, [b]From Ref [13]

TABLE – 4 Distances values between the more electronegative atoms for the stable conformations of trifluoridine

B3LYP/6-31G* method[a]			
Gas phase			
Distances (Å)	C1	C3	C5
F2-O8	3.009	3.051	3.041
F3-O8	3.066	3.025	3.031
O4-O6	2.760	2.904	3.617
O4-O5	2.968	3.087	2.966
N9-O7	2.295	2.311	2.297
N9-O4	2.363	2.345	2.362
N10-O7	2.297	2.289	2.295
N10-O8	2.285	2.284	2.284
Aqueous solution			
F2-O8	2.978	3.022	3.022
F3-O8	3.026	2.977	2.970
O4-O6	2.795	2.969	3.634
O4-O5	2.974	3.072	2.973
N9-O7	2.298	2.312	2.306
N9-O4	2.370	2.351	2.365
N10-O7	2.298	2.283	2.286
N10-O8	2.284	2.282	2.283

[a]This workHence, this study shows that C3 is the most stable conformer in both media probably due to the low repulsions between those electronegative atoms.

SOLVATION ENERGY

Table 5 shows the calculated uncorrected, corrected and the non electrostatic solvation energies for the five stable configurations of TFT at the B3LYP/6-31G* level of theory.

TABLE – 5 Calculated solvation energies (G) for the stable configurations of trifluridine

PCM/B3LYP/6-31G*[a]			
ΔG (kJ/mol)			
Trifluridine[a]			
Isomers	$\Delta G_u^{\#}$	ΔG_{ne}	ΔG_c
C1	-92.33	34.19	-126.52
C2	-86.82	35.32	-122.14
C3	-78.95	34.90	-113.85
C4	-87.61	34.53	-122.14
C5	-91.54	35.20	-126.74
Thymidine[b]			
C3	-86.56	29.59	-116.16

$\Delta G_c = \Delta G_{uncorrected}^{\#} - \Delta G_{Totalnon\text{-}electrostatic,}$

[a]This work, [b]From Ref [32]

The values are compared with the corresponding to the most stable C3 conformer of thymidine. Note that the higher differences between both antiviral agents are observed in the non electrostatic terms revealing that C1 and C5 present the lower values and that the C3 conformer of thymidine has approximately a similar value than the C3 isomer of TFT. Additionally, both structures do not evidence variations of volume in solution because the volumes for the C3 conformer of thymidine in both media are 257.3 $Å^3$ a similar value to the observed for C3 of TFT.

Here, differences were found between both structures when that isomer is compared with C3 of thymidine because it has a *Trans* conformation but when we analyzed the *Cis* conformation C3 of thymidine the dipole moment values are practically the same. This way, the higher dipole moment value and the little volume contraction observed in TFT in solution could be explained with these structures. In fact, the slight reduction of the bond lengths and angles of C3 could also explain the low volume contraction in solution, as observed in Table 2.

CHARGES, MOLECULAR ELECTROSTATIC POTENTIALS AND BOND ORDERS

The analysis of the charges is essential to understand the influence of the CF_3 groups on the properties of TFT. For this reason, in this work two charge's types, the atomic population natural (NPA) and those derived from the Merz-Kollman (MK) charges were calculated [38]. Both charges can be seen in **Tables 6** and 7. Analyzing the MK charges it is observed that the charges on the F3 atoms in the three isomers present the lower values in both media having on the C3 isomer the lowest value in solution than the other ones while the charges on the F1 atoms have the higher values in both media. In relation to the O atoms, the O4 atoms have the lower values while the values more negative are observed on the O5 atoms. The charges on the N9 atoms in the three isomers present the lower values in both media than on the N10 atoms. As expected, the charges on the H29 and H31 atoms have the higher values because they are attached to the O5 and O6 atoms whose charges in the three isomers have the most negative values. The NPA charges are slightly different from the MK charges having higher values in some cases such as, on the O5, O6, C20 and the three F atoms but they show approximately the same variations than the MK charges. Here, the differences with thymidine are clearly observed in the charges on the C atoms linked to the three H atoms of the CH_3 group because in thymidine the MK charges on C3 is -0.423 in gas phase while the NPA is -0.682 in the same medium while in TFT the two charge's types are positives because the C20 atoms are linked to the three F atoms.

TABLE – 6 Atomic MK charges for the three stable isomers of trifluridine in gas and aqueous solution phases

	B3LYP/6-31G*					
	MK' charges					
	Gas phase			Aqueous solution		
Atoms	C1	C3	C5	C1	C3	C5
1. F	-0.172	-0.167	-0.150	-0.161	-0.158	-0.148
2. F	-0.156	-0.146	-0.143	-0.155	-0.147	-0.151
3. F	-0.143	-0.138	-0.137	-0.144	-0.140	-0.143
4. O	-0.435	-0.397	-0.528	-0.398	-0.396	-0.469
5. O	-0.630	-0.621	-0.614	-0.621	-0.626	-0.600
6. O	-0.563	-0.576	-0.648	-0.559	-0.574	-0.646
7. O	-0.535	-0.536	-0.524	-0.535	-0.537	-0.528
8. O	-0.494	-0.492	-0.487	-0.498	-0.495	-0.485
9. N	-0.296	-0.233	-0.168	-0.289	-0.249	-0.108
10. N	-0.628	-0.629	-0.595	-0.620	-0.601	-0.574
11. C	0.434	0.258	0.438	0.336	0.292	0.224
12. C	0.081	0.176	0.147	0.075	0.217	0.200
13. C	-0.198	-0.296	-0.288	-0.236	-0.312	-0.354
14. C	0.320	0.237	0.462	0.274	0.200	0.388
15. C	-0.001	-0.017	0.037	0.001	0.023	0.042
16. C	0.184	0.169	0.072	0.232	0.166	0.036
17. C	0.685	0.704	0.624	0.686	0.695	0.634
18. C	-0.372	-0.339	-0.303	-0.375	-0.316	-0.254
19. C	0.681	0.673	0.649	0.676	0.651	0.614
20. C	0.469	0.434	0.419	0.453	0.419	0.422
21. H	0.048	0.118	0.039	0.089	0.108	0.125
22. H	0.044	0.063	0.042	0.056	0.054	0.043
23. H	0.065	0.105	0.068	0.084	0.108	0.099
24. H	0.090	0.109	0.113	0.107	0.107	0.133
25. H	0.102	0.076	-0.002	0.122	0.081	0.017
26. H	0.038	0.051	0.052	0.043	0.042	0.051
27. H	0.043	0.079	0.063	0.050	0.071	0.074
28. H	0.115	0.120	0.140	0.083	0.111	0.145
29. H	0.435	0.418	0.421	0.436	0.415	0.415
30. H	0.369	0.367	0.366	0.371	0.363	0.364
31. H	0.421	0.434	0.436	0.418	0.427	0.434

TABLE – 7 Atomic NPA charges for the three stable isomers of trifluridine in gas and aqueous solution phases

	B3LYP/6-31G*					
	NPA charges					
	Gas phase			Aqueous solution		
Atoms	C1	C3	C5	C1	C3	C5
1. F	-0.374	-0.375	-0.371	-0.371	-0.372	-0.367
2. F	-0.356	-0.354	-0.354	-0.357	-0.356	-0.356
3. F	-0.352	-0.353	-0.353	-0.354	-0.355	-0.354
4. O	-0.574	-0.592	-0.595	-0.574	-0.591	-0.590
5. O	-0.748	-0.755	-0.761	-0.747	-0.754	-0.756
6. O	-0.747	-0.774	-0.759	-0.746	-0.773	-0.758
7. O	-0.627	-0.619	-0.625	-0.629	-0.623	-0.624
8. O	-0.580	-0.579	-0.577	-0.586	-0.585	-0.581
9. N	-0.472	-0.469	-0.469	-0.467	-0.466	-0.466
10. N	-0.667	-0.669	-0.667	-0.658	-0.660	-0.659
11. C	0.284	0.275	0.287	0.282	0.274	0.278
12. C	0.073	0.073	0.072	0.072	0.072	0.073
13. C	-0.527	-0.524	-0.523	-0.526	-0.524	-0.523
14. C	0.047	0.046	0.054	0.044	0.043	0.052
15. C	-0.124	-0.119	-0.111	-0.125	-0.121	-0.111
16. C	0.074	0.082	0.080	0.079	0.084	0.084
17. C	0.832	0.838	0.834	0.829	0.835	0.832
18. C	-0.329	-0.323	-0.324	-0.325	-0.322	-0.316
19. C	0.668	0.670	0.668	0.659	0.662	0.661
20. C	1.131	1.131	1.131	1.130	1.131	1.130
21. H	0.256	0.264	0.254	0.260	0.266	0.267
22. H	0.222	0.228	0.237	0.224	0.230	0.236
23. H	0.250	0.261	0.250	0.249	0.261	0.248
24. H	0.269	0.252	0.268	0.268	0.253	0.261
25. H	0.265	0.256	0.232	0.267	0.259	0.226
26. H	0.193	0.209	0.208	0.194	0.211	0.209
27. H	0.213	0.220	0.222	0.214	0.222	0.222
28. H	0.285	0.276	0.277	0.277	0.273	0.266
29. H	0.478	0.477	0.482	0.477	0.476	0.480
30. H	0.452	0.452	0.453	0.456	0.456	0.457
31. H	0.487	0.492	0.482	0.485	0.493	0.481

The molecular electrostatic potentials (MEP) were also analyzed for the three isomers considered here because it is an important property to know the electronic distribution due to the presence in their structures of the CF_3 groups. The values are presented in **Table 8** while in **Figure 6** are shown the calculated electrostatic potential surfaces on the C3 isomers of TFT and thymidine in gas phase [32].

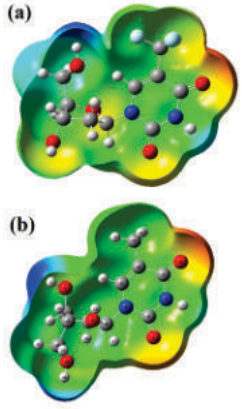

Figure 6. Calculated electrostatic potential surfaces on the molecular surfaces of the C3 structures of: (a) trifluridine and (b) thymidine. Color ranges, in au: from red -0.071 to blue + 0.071. B3LYP functional and 6-31G* basis set. Isodensity value of 0.005.

These figures do not present differences in the colorations but the MEP values shows a higher value on the C13 atom belonging to the CH_3 group of thymidine (-14.742 a.u.) while in TFT the C20 atoms belonging to the CF_3 group of the three isomers have a lower value (-14.478 a.u.). Moreover, the MEP values observed on the two N atoms in thymidine have higher values than the corresponding to TFT. Thus, the CF_3 group has influence notable on the pyrimidine ring than on the sugar ring. The different colours indicate clearly the nucleophilic and electrophilic sites reacting with potentials biological electrophiles or nucleophiles, respectively. Here, both antiviral agents present practically the same colorations but the MEP values support a higher electronic density on the pyrimidine ring of thymidine, as compared with trifluridine.

In **Table 9** are presented the bond order (BO) values expressed as Wiberg indexes for the three isomers of trifluridine in the two media. When these values are analyzed exhaustively and compared with the values corresponding to the C3 conformer of thymidine [32] we observed that the C13 atom belonging to the CH_3 group (3.834) has a higher BO than the C20 atom belonging to the CF_3 group (3.670) of the C3 isomer of TFT. Besides, the BO values for the N atoms belonging to the glycosyl bonds and for the C atoms attached to the CH_3 or CF_3 groups are slightly different between them while the C atoms involved in the glycosyl bonds have practically the same values. Thus, for C3 of TFT the BO values are N9= 3.398 and C11=3.793 while for C3 of thymidine are N5= 3.385 and C16=3.794. On the other hand, the BO values for the atoms belonging to the sugar ring present few variations when the CH_3 group is changed by the CF_3 group. This way, the high polarization coefficients that present the CF bonds (0.51210.8589) in TFT, in relation to the CH reveals (0.78540.6190) an of the principal difference between both antiviral agents

NBO AND QAIM STUDIES

The above studies have showed that some properties such as, the atomic charges and the MEP values change when the CH_3 group is replaced by the CF_3 group. For theses reasons, the stabilities of the three isomers of TFT were evaluated in both media at the B3LYP/6-31G* level of theory by using NBO and QAIM calculations [27,28]. Thus, the main delocalization energy values for the three isomers most stable of TFT can be seen in **Table 10**. The results for the three isomers show three different delocalizations which are attributed to the $\Delta ET_{\pi\rightarrow\pi^*}$, $\Delta ET_{n\rightarrow\sigma^*}$ and $\Delta ET_{n\rightarrow\pi^*}$ charge transfers. The former are related to the C=C bonds of the pyrimidine rings while the two remains are related to the lone pairs of the F, O and N atoms. Note that the charge transfers due to the N atoms are the higher contributions to the ΔE_{Total}.

TABLE – 8 Molecular electrostatic potential (in a.u.) for the three isomers of trifluridine

	B3LYP/6-31G*					
	Gas phase			Aqueous solution		
Atoms	C1	C3	C5	C1	C3	C5
1. F	-26.524	-26.524	-26.525	-26.519	-26.518	-26.519
2. F	-26.534	-26.535	-26.535	-26.536	-26.538	-26.536
3. F	-26.535	-26.535	-26.535	-26.538	-26.538	-26.537
4. O	-22.279	-22.289	-22.276	-22.279	-22.288	-22.279
5. O	-22.290	-22.294	-22.291	-22.288	-22.293	-22.291
6. O	-22.287	-22.278	-22.301	-22.287	-22.276	-22.301
7. O	-22.322	-22.326	-22.321	-22.322	-22.328	-22.322
8. O	-22.334	-22.335	-22.333	-22.337	-22.339	-22.334
9. N	-18.264	-18.266	-18.260	-18.260	-18.264	-18.257
10. N	-18.284	-18.287	-18.283	-18.281	-18.285	-18.279
11. C	-14.616	-14.627	-14.616	-14.614	-14.625	-14.617
12. C	-14.653	-14.660	-14.660	-14.651	-14.657	-14.658
13. C	-14.709	-14.717	-14.713	-14.705	-14.713	-14.706
14. C	-14.663	-14.665	-14.665	-14.660	-14.663	-14.662
15. C	-14.661	-14.664	-14.679	-14.660	-14.661	-14.677
16. C	-14.657	-14.659	-14.651	-14.653	-14.657	-14.644
17. C	-14.573	-14.576	-14.571	-14.571	-14.575	-14.569
18. C	-14.706	-14.707	-14.704	-14.704	-14.706	-14.699
19. C	-14.610	-14.612	-14.609	-14.611	-14.613	-14.608
20. C	-14.478	-14.478	-14.478	-14.477	-14.478	-14.476
21. H	-1.090	-1.097	-1.091	-1.089	-1.095	-1.088
22. H	-1.087	-1.097	-1.095	-1.084	-1.094	-1.094
23. H	-1.082	-1.091	-1.084	-1.077	-1.087	-1.077
24. H	-1.083	-1.086	-1.087	-1.079	-1.083	-1.077
25. H	-1.094	-1.096	-1.099	-1.091	-1.093	-1.095
26. H	-1.089	-1.093	-1.113	-1.084	-1.092	-1.110
27. H	-1.091	-1.093	-1.112	-1.090	-1.089	-1.113
28. H	-1.058	-1.059	-1.052	-1.053	-1.055	-1.043
29. H	-0.971	-0.975	-0.971	-0.969	-0.974	-0.971
30. H	-0.982	-0.985	-0.980	-0.977	-0.982	-0.976
31. H	-0.970	-0.962	-0.982	-0.970	-0.959	-0.982

TABLE – 9 Wiberg indexes for the three isomers of trifluridine

	B3LYP/6-31G*					
	Wiberg indexes					
	Gas phase			Aqueous solution		
Atoms	C1	C3	C5	C1	C3	C5
1. F	1.002	0.999	1.006	1.008	1.006	1.012
2. F	1.029	1.032	1.032	1.027	1.028	1.028
3. F	1.036	1.034	1.034	1.030	1.029	1.031
4. O	2.028	2.001	1.999	2.022	1.999	1.998
5. O	1.798	1.790	1.788	1.795	1.788	1.790
6. O	1.800	1.779	1.776	1.795	1.781	1.774
7. O	1.992	2.004	1.994	1.985	1.994	1.992
8. O	2.031	2.032	2.034	2.014	2.016	2.019
9. N	3.403	3.398	3.403	3.408	3.402	3.405
10. N	3.236	3.234	3.237	3.244	3.242	3.243
11. C	3.802	3.793	3.798	3.801	3.792	3.793
12. C	3.869	3.863	3.860	3.869	3.864	3.862
13. C	3.887	3.888	3.886	3.888	3.888	3.889
14. C	3.844	3.851	3.845	3.844	3.852	3.851
15. C	3.821	3.803	3.804	3.823	3.804	3.806
16. C	3.854	3.860	3.867	3.860	3.860	3.877
17. C	3.871	3.869	3.870	3.872	3.871	3.871
18. C	3.967	3.969	3.969	3.967	3.969	3.971
19. C	3.901	3.901	3.901	3.906	3.905	3.906
20. C	3.670	3.670	3.672	3.672	3.670	3.674
21. H	0.938	0.935	0.940	0.936	0.934	0.933
22. H	0.954	0.951	0.947	0.953	0.950	0.947
23. H	0.940	0.934	0.940	0.940	0.934	0.941
24. H	0.930	0.938	0.930	0.930	0.938	0.934
25. H	0.933	0.937	0.950	0.932	0.936	0.953
26. H	0.966	0.959	0.960	0.965	0.959	0.959
27. H	0.958	0.955	0.955	0.957	0.954	0.955
28. H	0.925	0.930	0.927	0.930	0.932	0.933
29. H	0.774	0.774	0.769	0.774	0.775	0.771
30. H	0.799	0.799	0.799	0.796	0.796	0.795
31. H	0.765	0.759	0.769	0.766	0.758	0.770

TABLE – 10 Main delocalization energy (in kJ/mol) for the three isomers of trifluridine

Delocalization	B3LYP/6-31G* method[a]							
	Trifluridine						Thymidine[a]	
	Gas phase			Aqueous solution			Gas	PCM
	C1	C3	C5	C1	C3	C5	C3	C3
*πC16-C18→π*O8-C19*	103.60	101.95	101.49	107.34	105.92	103.12	98.44	102.58
ΔET$_{π→π*}$	**103.6**	**101.95**	**101.49**	**107.34**	**105.92**	**103.12**	**98.44**	**102.58**
*LP(3)F1 → σ*F2-C20*	46.10	43.85	45.44	46.82	45.23	45.14		
*LP(3)F1 → σ*F3-C20*	42.84	44.77	44.85	44.98	46.40	47.53		
*LP(3)F2 → σ*F1-C20*	56.93	57.31	56.55	53.80	54.13	53.29		
*LP(3)F2 → σ*F3-C20*	39.71	40.21	40.80	40.59	40.63	41.13		
*LP(3)F3 → σ*F1-C20*	57.39	57.39	56.64	53.96	53.92	53.00		
*LP(3)F3 → σ*F2-C20*	41.09	40.59	41.17	40.71	40.92	41.76		
*LP(2)O4 → σ*N9-C11*	50.49	26.79	39.79	47.53	30.05	41.67	115.33	109.39
*LP(2)O7 → σ*N9-C17*	116.24	119.05	117.54	112.94	114.41	114.41	107.43	102.49
*LP(2)O7 → σ*N10-C17*	107.30	108.30	107.09	104.04	104.46	104.12	25.71	25.54
*LP(2)O8 → σ*N10-C19*	126.69	125.52	126.78	116.24	115.87	115.95	39.21	37.03
*LP(2)O8 → σ*C18-C19*	84.52	84.98	84.89	79.80	80.51	80.88	122.01	113.19
*LP(2)O31 → σ*C9-C10*							77.71	73.40
ΔET$_{n→σ*}$	**769.3**	**748.76**	**761.54**	**741.41**	**726.53**	**738.88**	**487.4**	**461.04**
*LP(1)N9→ π*O7-C17*	236.17	229.23	232.99	241.69	236.04	238.38	242.73	256.98
*LP(1)N9→ π*C16-C18*	190.61	183.96	189.73	194.45	185.63	189.60	152.61	154.62
*LP(1)N10→ π*O7-C17*	268.52	262.21	268.86	270.02	264.55	267.44	255.23	261.54
*LP(1)N10→ π*O8-C19*	203.27	206.53	203.11	217.15	219.11	218.20	213.18	223.42
ΔET$_{n→π*}$	**898.57**	**881.93**	**894.69**	**923.31**	**905.33**	**913.62**	**863.75**	**896.56**
*π*C9-O31→ π*C10-C11*							401.50	391.33
ΔET$_{π*→π*}$							**401.5**	**391.33**
ΔETotal	**1771.47**	**1732.64**	**1757.72**	**1772.06**	**1737.78**	**1755.62**	**1851.09**	**1851.51**

Here, the higher values observed for C1 could justify the presence of this isomer in both media. When these delocalizations are compared with the values for C3 of thymidine calculated in this work, we observed five significant differences: (i) the $\Delta ET_{\pi\rightarrow\pi^*}$ charge transfers are slightly higher in trifluridine, (ii) the $\Delta ET_{n\rightarrow\sigma^*}$ charge transfers are higher in trifluridine, (iii) the $\Delta ET_{n\rightarrow\pi^*}$ charge transfers are higher in trifluridine, (iv) the $\Delta ET_{\pi^*\rightarrow\pi^*}$ charge transfers are only observed in thymidine and finally, (v) the resultant ΔE_{Total} is higher for thymidine than TFT. The latter result could probably justify in part the different biological properties observed for thymidine than TFT.

The possible presences of intra-molecular interactions in the three isomers of TFT were also investigated by using the topological properties in order to analyze their stabilities in both media. This way, the electron density distribution, $\rho(r)$, the Laplacian, $\nabla^2\rho(r)$, the eigenvalues $(\lambda 1, \lambda 2, \lambda 3)$ of the Hessian matrix and, the $\lambda 1/\lambda 3$ ratio are parameters that calculated in the bond critical points (BCPs) can explain the nature of the interactions. For instance, a interaction is covalent when $\lambda 1/\lambda 3 > 1$, $\nabla^2\rho(r) < 0$ and has high values of $\rho(r)$ and $\nabla^2\rho(r)$ while if $\lambda 1/\lambda 3 < 1$ and $\nabla^2\rho(r) > 0$ the interaction is of hydrogen bonds, ionic or highly polar covalent [39]. In **Table 11** are summarized those parameters for the interactions observed in the C1 and C5 isomers of TFT while in **Table 12** are presented those interactions observed in C3. For C1 in both media are observed two BCPs (O4---H28 and O6---H28) and their corresponding RCPs and, the RCPs of the pyrimidine and sugar rings (RCP_B= base RCP_S = sugar). On the contrary, for C5 in gas phase is observed a BCP (O4---H28) while there isn't observed BCP for this isomer in solution. Note that for the most stable isomer, C3, three BCPs are observed in both media with their three corresponding RCPs and, the expected RCP_B and RCP_S. Hence, we observed that C3 is the most stable isomer in both media due to the higher quantity of H bonds formed that confers to it a higher stability. Also, the most stable C3 conformer of thymidine exhibit three H bonds. On the other hand, when the $\rho(r)$ and $\nabla^2\rho(r)$ values of RCP_B and RCP_S are represented in function of the isomers of TFT in **Figure 7** the lowest values of those two properties are observed in C3. The $\rho(r)$ and $\nabla^2\rho(r)$ values are higher in RCP_S and, moreover, these points present the higher modifications. When these values are compared with those observed for C3 of thymidine [32], these are, RCP_B [$\rho(r)$ = 0.0190 a.u. and $\nabla^2\rho(r)$ = 0.1483 a.u.] and RCP_S [$\rho(r)$ = 0.0387 a.u. and $\nabla^2\rho(r)$ = 0.2756 a.u.] we observed higher values in TFT, especially in RCP_S [$\rho(r)$ = 0.0391 a.u. and $\nabla^2\rho(r)$ = 0.2784 a.u.]. Here, the slightly increase in the density and Laplacian values observed for both rings of C3 do not justify the higher reactivity of thymidine than TFT.

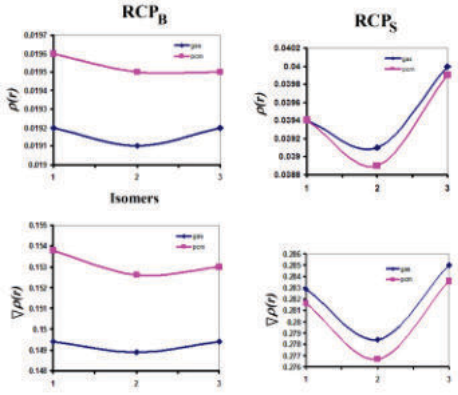

Figure 7. Variations of the $\rho(r)$ and $\nabla^2\rho(r)$ values in the RCP_B and RCP_S for the C1, C3 and C5 isomers of trifluridine in gas and aqueous solution phases at B3LYP/6-31G* level of theory.

HOMO-LUMO AND DESCRIPTORS STUDIES

The frontier orbitals are of interest to predict the reactivity and, also, to predict the behaviours of the isomers of TFT in the two different media studied by using some practical descriptors [29-36]. For these reasons, for the C1, C3 and C5 isomers of TFT in both media were calculated the HOMO and LUMO orbitals, energy band gaps, chemical potential (μ), electronegativity (χ), global hardness (η), global softness (S) and global electrophilicity index (ω).

TABLE – 11 An Analysis of the Bond Critical points (BCP) and Ring Critical Points (RCP) for the C1 and C5 isomers of trifluridine

B3LYP/6-31G*						
C1						
Gas phase						
Parameter (a.u.)	O4---H28	RCP1	O6---H28	RCP2	RCP_B	RCP_S
$\rho(r_c)$	0.0191	0.0186	0.0138	0.0095	0.0192	0.0394
$\nabla^2\rho(r_c)$	0.0793	0.0987	0.0439	0.0383	0.1494	0.2829
λ_1	-0.0201	-0.0174	-0.0152	-0.0075	-0.0145	-0.0435
λ_2	-0.0100	0.0138	-0.0150	0.0190	0.0660	0.1609
λ_3	0.1096	0.1022	0.0741	0.0268	0.0978	0.1654
$\lvert\lambda_1\rvert/\lambda_3$	0.1834	0.1703	0.2051	0.2799	0.1483	0.2630
Distances (Å)	2.243		2.317			
Aqueous solution						
Parameter (a.u.)	O4---H28	RCP1	O6---H28	RCP2	RCP_B	RCP_S
$\rho(r_c)$	0.0183	0.0180	0.0112	0.0085	0.0196	0.0394
$\nabla^2\rho(r_c)$	0.0772	0.0929	0.0364	0.0348	0.1538	0.2816
λ_1	-0.0186	-0.0166	-0.0117	-0.0059	-0.0151	-0.0432
λ_2	-0.0080	0.0105	-0.0110	0.0161	0.0696	0.1598
λ_3	0.1040	0.0989	0.0590	0.0245	0.0992	0.1650
$\lvert\lambda_1\rvert/\lambda_3$	0.1788	0.1678	0.1983	0.2408	0.1522	0.2618
Distances (Å)	2.272		2.422			
C5						
	Gas phase				Aqueous solution	
Parameter (a.u.)	O4---H28	RCP1	RCP_B	RCP_S	RCP_B	RCP_S
$\rho(r_c)$	0.0192	0.0184	0.0192	0.0400	0.0195	0.0399
$\nabla^2\rho(r_c)$	0.0770	0.0997	0.1494	0.2850	0.1530	0.2836
λ_1	-0.0204	-0.0171	-0.0145	-0.0437	-0.0149	-0.0433
λ_2	-0.0116	0.0164	0.0656	0.1636	0.0690	0.1623
λ_3	0.1095	0.1004	0.0982	0.1651	0.0988	0.1645
$\lvert\lambda_1\rvert/\lambda_3$	0.1863	0.1703	0.1477	0.2647	0.1508	0.2632
Distances (Å)	2.239					

RCP1= new1; RCP2= new1; RCP_B= base RCP_S = sugar

TABLE – 12 An Analysis of the Bond Critical points (BCP) and Ring Critical Points (RCP) for the C3 isomer of trifluridine

C3								
Gas phase								
Parameter	O6---H23	RCP1	O6---H28	RCP2	O7---H21	RCP3	RCP_B	RCP_S
$\rho(r_c)$	0.0091	0.0082	0.0163	0.0052	0.0182	0.0181	0.0191	0.0391
$\nabla^2\rho(r_c)$	0.0358	0.0387	00477	0.0230	0.0761	0.0915	0.1489	0.2784
λ_1	-0.0072	-0.0043	-0.0193	-0.0017	-0.0186	-0.0174	-0.0144	-0.0437
λ_2	-0.0054	0.0071	-0.0186	0.0078	-0.0070	0.0086	0.0645	0.1590
λ_3	0.0484	0.0358	0.0857	0.0169	0.1018	0.1004	0.0987	0.1630
$\lvert\lambda_1\rvert/\lambda_3$	0.1488	0.1201	0.2252	0.1006	0.1827	0.1733	0.1459	0.2681
Distances	2.569		2.244		2.267			
Aqueous solution								
Parameter	O6---H23	RCP1	O6---H28	RCP2	O7---H21	RCP3	RCP_B	RCP_S
$\rho(r_c)$	0.0083	0.0077	0.0190	0.0057	0.0179	0.0177	0.0195	0.0389
$\nabla^2\rho(r_c)$	0.0330	0.0357	0.0539	0.0244	0.0738	0.0892	0.1526	0.2767
λ_1	-0.0062	-0.0040	-0.0233	-0.0029	-0.0183	-0.0171	-0.0149	-0.0434
λ_2	-0.0046	0.0062	-0.0225	0.0078	-0.0071	0.0087	0.0682	0.1572
λ_3	0.0438	0.0335	0.0997	0.0195	0.0992	0.0976	0.0992	0.1629
$\lvert\lambda_1\rvert/\lambda_3$	0.1416	0.1194	0.2337	0.1487	0.1845	0.1752	0.1502	0.2664
Distances	2.618		2.174		2.276			

RCP1= new1; RCP2= new1; RCP_B= base RCP_S = sugar

The results together with the equations used to calculate the descriptors can be seen in Table 13 compared with the values calculated for thymidine, at the B3LYP/6-31G* level of theory and, for idoxuridine at the B3LYP/3-21G* calculations. First, comparing the three isomers of TFT we observed that C5 is the most reactive isomer of TFT in both media and, comparing with thymidine, their C3 conformer has higher reactivity than TFT but, idoxuridine is most reactive than thymidine and TFT. Evidently, the presence of the CF3 group in the pyrimidine rings of TFT increase their gap values diminishing their reactivities while the iodine atom in the pyrimidine ring of idoxuridine decrease the gap value and, as a consequence increase their reactivity. Notice that the reactivity of all the antiviral agents presented in Table 13 increase notably their values in solution. On the other hand, the incorporation of a CF3 group or of an iodine atom in the pyrimidine rings increases the electrophilicity and nucleophilicity indexes in TFT and idoxuridine, as compared with thymidine. Evidently in idoxuridine, the iodine atom generate the activation of the two rings and, consequently increase the values of RCP_B [$\rho(r)$ =0.0217 a.u. and $\nabla^2\rho(r)$ = 0.1280 a.u.] and RCP_S $\Delta[\rho(r) = 0.0375$ a.u. and $\Delta^2(r) = 0.2368$ a.u.] which justify the increase in the reactivity.

NMR STUDY

In this study, the ^{1}H-NMR and ^{13}C-NMR spectra for the three isomers of TFT in aqueous solution were predicted by using the GIAO method [37] at the B3LYP/6-31G* level of theory. The calculated chemical shifts for the hydrogen and carbon nuclei of the C1, C3 and C5 isomers of TFT are summarized in Table 14 and 15, respectively and, both results were compared with the experimental values corresponding to TFT and thymidine [32]. For the hydrogen nuclei was observed a reasonable correlation with both experimental values showing RMSD values between 2.59 and 2.35 ppm while for the carbon nuclei the correlation is not very good due to that the theoretical values are underestimate. Table 15 shows that the calculated values for the C20 atoms belong to the CF_3 groups of the isomers of TFT are between 135.90 and 135.37 ppm, as expected due to the electronegativity of the F atoms while in thymidine a bigger shift of the corresponding signal towards lower fields is expected (12.34 ppm) due to the CH_3 group. The differences between experimental and theoretical values could be easily attributed to the B3LYP/6-31G* calculations, to the solvent and, to the different molecule compared.

TABLE – 14 Calculated hydrogen chemical shifts (δ, in ppm) for the C1, C3 and C5 isomers of trifluridine in aqueous solution

Atoms	B3LYP/6-31G*Method[a]		Experimental		
	Trifluridine		Trifluridine[b]		Thymidine[c]
	C1	C3	C5	DMSO-d6[d]	DMSO-d6[d]
21-H	6.54	6.95	6.72	6.2	6.18
22-H	4.44	5.05	4.91	4.3	4.26
23-H	2.00	2.57	2.01	2.2	2.08
24-H	2.87	2.23	2.56	2.2	2.08
25-H	5.06	4.55	4.78	3.8	3.78
26-H	3.63	4.30	4.36	3.6	3.55
27-H	4.20	4.37	4.67	3.6	3.60
28-H	8.49	9.01	7.66	8.8	7.71
29-H	0.67	0.71	0.66	5.25	5.25
30-H	6.70	6.70	6.72	11.8	11.3
31-H	1.11	1.14	0.57	5.25	5.04
RMSD[b]	**2.46**	**2.46**	**2.59**		
RMSD[c]	**2.35**	**2.37**	**2.45**		

TABLE – 15 Calculated carbon chemical shifts (δ, in ppm) for the C1, C3 and C5 isomers of trifluridine in aqueous solution

Atoms	B3LYP/6-31G* Method[a] Trifluridine			Experimental Thymidine[b]
	C1	C3	C5	D_2O[b]
11-C	100.09	96.33	97.23	85.88
12-C	84.28	85.19	82.02	71.26
13-C	55.38	54.65	55.31	39.36
14-C	96.63	95.96	93.76	87.34
15-C	73.53	75.07	69.97	62.01
16-C	143.51	146.69	143.00	138.28
17-C	150.89	151.24	150.77	152.42
18-C	112.16	113.41	113.77	112.17
19-C	160.18	159.85	159.71	167.17
20-C	135.90	135.78	135.37	12.34[#]
RMSD[b]	10.14	10.05	8.74	

TABLE – 13

Calculated HOMO and LUMO orbitals, energy band gap, chemical potential (μ), electronegativity (χ), global hardness (η), global softness (S) and global electrophilicity index (ω) for the most stable isomers of trifluridine

B3LYP method					
6-31G*					3-21G*
Trifluridine[a]				Thymidine[b]	Idoxuridine[a]
Gas phase[a]					
Orbitals	C1	C3	C5	C3	C5
HOMO	-6.9138	-6.8882	-6.9459	-6.1061	-6.2600
LUMO	-1.3345	-1.3006	-1.3766	-0.6313	-1.2438
GAP	-5.5793	-5.5876	-5.5693	-5.4748	-5.0162
Descriptors					
χ	-2.7897	-2.7938	-2.7847	-2.7374	-2.5081
μ	-4.1242	-4.0944	-4.1613	-3.3687	-3.7519
η	2.7897	2.7938	2.7847	2.7374	2.5081
S	0.1792	0.1790	0.1796	0.1826	0.1994
ω	3.0485	3.0002	3.1092	2.0728	2.8063
E	-11.5049	-11.4389	-11.5876	-9.2215	-9.4101
Aqueous solution[a]					
Orbitals	C1	C3	C5	C3	C5
HOMO	-6.9621	-6.9621	-7.0413	-6.1128	-6.2613
LUMO	-1.4443	-1.4443	-1.5627	-0.6800	-1.2703
GAP	-5.5178	-5.5178	-5.4786	-5.4328	-4.991

	Descriptors				
χ	-2.7589	-2.7589	-2.7393	-2.7164	-2.4955
μ	-4.2032	-4.2032	-4.3020	-3.3964	-3.7658
η	2.7589	2.7589	2.7393	2.7164	2.4955
S	0.1812	0.1812	0.1825	0.1841	0.2004
ω	3.2018	3.2018	3.3781	2.1233	2.8414
E	-11.5962	-11.5962	-11.7845	-9.2260	-9.3976

χ = - [E(LUMO)- E(HOMO)]/2, μ = [E(LUMO) + E(HOMO)]/2; η = [E(LUMO) – E(HOMO)]/2, $S = \frac{1}{2}\eta$, $\omega = \mu^2/2\eta$, E= (eV)

[a]This work

[b]From Ref [32]

VIBRATIONAL STUDY

To perform this analysis we have considered the three most stable isomers of TFT and their infrared and Raman spectra were compared with the corresponding to thymidine because the only difference of TFT with it is the presence in their structure of a CH_3 group. The three isomers of TFT, as thymidine, have 87 normal vibration modes which are active in both IR and Raman spectra. Figure 8 shows the experimental IR spectrum of thymidine in the 4000-2500 cm^{-1} region take from Ref [42] compared with the corresponding predicted for the three isomers of TFT.

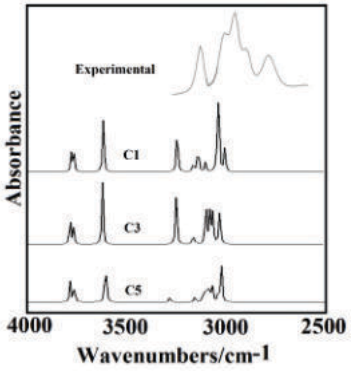

Figure 8. Comparison between the experimental infrared spectra of thymidine in the 3300-2900 cm^{-1} region, taken from Ref [32], with the corresponding predicted by B3LYP/6-31G* calculations for the C1, C3 and C5 isomers of trifluoridine in gas phase.

The IR predicted spectra of those three isomers are compared in **Figure 9** with the corresponding to thymidine at B3LYP/6-31G* level of theory. In the IR spectra of thymidine is notable the strong intensities of the bands associated to the CH_3 stretching and deformation modes in the 3100-2900 and 1900-1700 cm^{-1} regions while in the three isomers of TFT the CF_3 stretching and deformation modes are associated with IR and Raman bands in the 1200-20 cm^{-1} region. The Raman predicted for thymidine and the three isomers are observed in **Figure 10**. In both Figures is notable the increase in the intensities of the bands attributed to the N-H and C-H stretching modes of the pyrimidine rings of the three isomers of TFT due to the CF_3 groups.

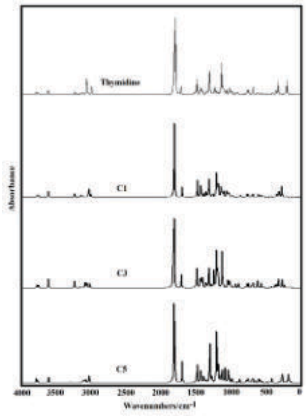

Figure 9. Comparisons between the predicted infrared spectra of thymidine with the corresponding ones for the C1, C3 and C5 isomers of trifluoridine in gas phase at B3LYP/6-31G* level of theory.

ASSIGNMENTS

OH and NH modes. The SQM calculations predicted the OH stretching modes at higher wavenumbers than the NH stretching modes, this way these modes are assigned as predicted by calculations. The OH in-plane deformation modes are predicted between 1224 and 1157 cm^{-1} while in thymidine these modes were assigned to the bands at 1288, 1197 and 1173 cm^{-1}. Hence, it is notable the shifting of these modes due to the CF_3 group. The NH rocking modes in the C3 conformer of thymidine was predicted at 1346 cm^{-1} while in the isomers of TFT are predicted between 1389 and 1370 cm^{-1}. In thymidine, the OH out-of-plane deformation modes were assigned at 298, 276 and 180 cm^{-1} while for the three isomers of TFT these modes can be assigned to the bands between 300 and 165 cm^{-1}.

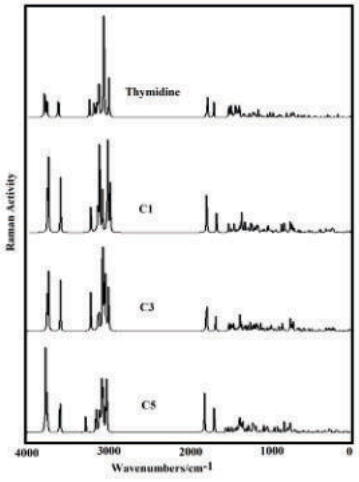

Figure 10. Comparisons between the predicted Raman spectra of thymidine with the corresponding ones for the C1, C3 and C5 isomers of trifluoridine in gas phase at B3LYP/6-31G* level of theory.

Figures 11 and **12** show the comparisons among the experimental Raman spectrum of thymidine in the 2000-1000 and 1000-0 cm^{-1} regions with those corresponding to the three isomers of TFT predicted at B3LYP/6-31G* level of theory. The comparisons between the IR spectra of the most stable isomers C3 of thymidine and trifluridine, shown in **Figure 13**, show clearly the differences between both antiviral agents due to the presence of the CH_3/CF_3 groups. The experimental bands for thymidine and the calculated wavenumbers for the C1, C3 and C5 isomers of trifluridine in gas phase and aqueous solution together with the corresponding assignments are presented in **Table 14.** The assignments were performed by comparison with those reported for thymidine [32] and with the results of the SQM calculations preformed here. Brief discussions of the assignments for some groups are presented below.

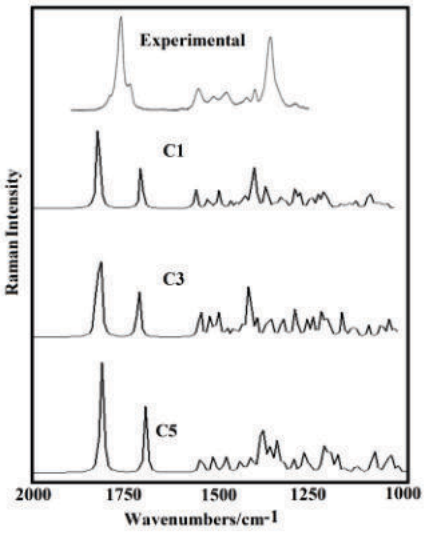

Figure 11. Comparison between the experimental infrared spectra of thymidine in the 2000-1000 cm^{-1} region, taken from Ref [32], with the corresponding predicted by B3LYP/6-31G* calculations for the C1, C3 and C5 isomers of trifluoridine in gas phase.

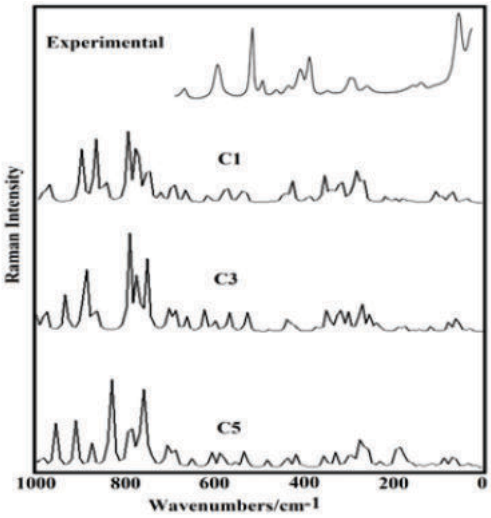

Figure 12. Comparison between the experimental infrared spectra of thymidine in the 1000-0 cm^{-1} region, taken from Ref [32], with the corresponding predicted by B3LYP/6-31G* calculations for the C1, C3 and C5 isomers of trifluoridine in gas phase.

TABLE – 14 Observed and calculated wavenumbers (cm^{-1}) and assignments for the C1, C3 and C5 isomers of trifluridine in gas phase and aqueous solution

Experimental[b]		B3LYP/6-31G*[a]											
		C1				C3				C5			
		Gas phase		Aqueous solution		Gas phase		Aqueous solution		Gas phase		Aqueous solution	
IR[c]	Raman[c]	SQM[d]	Asignment	SQM[d]	Asignment	SQM[d]	Asignment	SQM[d]	Asignment	SQM[d]	Asignment	SQM[d]	Asignment
		3603	νO6-H31	3588	νO6-H31	3607	νO6-H31	3585	νO6-H31	3620	νO6-H31	3590	νO6-H31
3482	3306 (10)	3590	νO5-H29	3573	νO5-H29	3588	νO5-H29	3570	νO5-H29	3599	νO5-H29	3584	νO5-H29
3130	3157 (1)	3451	νN10-H30	3423	νN10-H30	3451	νN10-H30	3422	νN10-H30	3451	νN10-H30	3412	νN10-H30
3075	3092 (9)	3096	νC16-H28	3116	νC16-H28	3096	νC16-H28	3065	νC16-H28	3142	νC16-H28	3137	νC16-H28
		3020	$\nu_a CH_2$(C13)	3031	$\nu_a CH_2$(C13)	3017	νC11-H21	3035	$\nu_a CH_2$(C13)	3024	$\nu_a CH_2$(C13)	3032	νC11-H21
2970	2967 (63)	2998	νC14-H25	3009	νC11-H21	3002	$\nu_a CH_2$(C13)	3020	νC11-H21	2984	νC11-H21	3019	$\nu_a CH_2$(C13)
2964	2956 (55)	2991	νC11-H21	2991	νC14-H25	2960	$\nu_s CH_2$(C13)	2978	$\nu_s CH_2$(C13)	2968	$\nu_a CH_2$(C15)	2968	$\nu_s CH_2$(C13)
2934	2935 (40)	2959	$\nu_s CH_2$(C13)	2976	$\nu_s CH_2$(C13)	2952	νC14-H25	2966	νC14-H25	2952	$\nu_s CH_2$(C13)	2963	$\nu_a CH_2$(C15)
2902	2905 (14)	2901	$\nu_a CH_2$(C15)	2951	$\nu_a CH_2$(C15)	2935	$\nu_a CH_2$(C15)	2960	$\nu_a CH_2$(C15)	2938	νC12-H22	2957	νC12-H22
	2861 (10)	2893	νC12-H22	2947	νC12-H22	2921	νC12-H22	2953	νC12-H22	2908	νC14-H25	2929	νC14-H25
	2760 (4)	2868	$\nu_s CH_2$(C15)	2910	$\nu_s CH_2$(C15)	2888	$\nu_s CH_2$(C15)	2909	$\nu_s CH_2$(C15)	2895	$\nu_s CH_2$(C15)	2914	$\nu_s CH_2$(C15)
1748	1810 (2)	1748	νC19=O8	1684	νC17=O7	1756	νC17=O7	1688	νC17=O7	1750	νC19=O8	1686	νC17=O7
1700	1690 (15)	1744	νC17=O7	1647	νC19=O8	1747	νC19=O8	1655	νC19=O8	1746	νC17=O7	1649	νC19=O8
	1643 (40)	1636	νC16-C18	1626	νC16-C18	1648	νC16-C18	1637	νC16-C18	1637	νC16-C18	1630	νC16-C18
1478		1492	δCH_2(C15)	1485	$wagCH_2$(C15)	1474	νN9-C16 δCH_2(C15)	1469	δCH_2(C15)	1486	δCH_2(C15)	1476	δCH_2(C15)
	1459 (15)	1454	$wagCH_2$(C15)	1464	δCH_2(C15)	1451	ρ'C11-H21	1458	νN9-C16	1449	$wagCH_2$(C15)	1457	νN9-C16
1456		1443	δCH_2(C13)	1456	νN9-C16	1444	δCH_2(C13)	1435	δCH_2(C13)	1447	δCH_2(C13)	1451	$wagCH_2$(C15)
1435	1437 (23)	1439	νN9-C16	1432	δCH_2(C13)	1430	$wagCH_2$(C15)	1430	$wagCH_2$(C15)	1441	νN9-C16	1427	δCH_2(C13)
1402	1404 (13)	1403	ρC'12-H22	1410	ρ'C11-H21	1402	ρC'12-H22	1413	βC16-H28	1410	ρC'12-H22	1403	ρ'C11-H21
1392 sh	1391 (23)	1398	νC18-C20	1404	ρC'12-H22	1398	νC18-C19	1407	ρC'12-H22	1399	ρ'C11-H21	1399	ρC'12-H22
		1383	βN10-H30	1386	βN10-H30	1383	βN10-H30	1389	βN10-H30	1386	ρ'C14-H25	1377	βN10-H30
	1366 (100)	1372	ρC14-H25	1383	ρC14-H25	1368	ρC11-H21	1370	βN10-H30	1380	βN10-H30	1376	ρC14-H25
1363		1348	βC16-H28	1350	βC16-H28	1364	βC16-H28	1368	ρC11-H21	1352	ρC11-H21	1358	ρC11-H21
1352	1353 (35)	1340	ρ'C11-H21	1346	ρC11-H21	1347	ρC14-H25	1347	ρC14-H25	1341	ρC14-H25	1353	βC16-H28
1319	1325 (6)	1321	ρC11-H21	1327	$wagCH_2$(C13) ρC12-H22	1327	$wagCH_2$(C13) ρC12-H22	1333	$wagCH_2$(C13)	1328	βC16-H28	1330	$wagCH_2$(C13)
	1292 (3)	1304	ρC12-H22	1305	ρ'C14-H25	1314	ρ'C14-H25	1316	ρ'C14-H25	1306	ρC12-H22	1306	ρ'C14-H25
1288		1288	ρ'C11-H21	1296	νN9-C16	1302	$\delta_s CF_3$	1294	ρC12-H22	1294	νC18-C20	1299	νC18-C20
1277	1279 (5)	1269	$wagCH_2$(C13)	1273	$wagCH_2$(C13)	1278	νC18-C20	1274	νC18-C20	1268	$wagCH_2$(C13)	1280	ρC12-H22
1253		1263	νC18-C20	1262	νC18-C20	1267	$wagCH_2$(C13) ρCH_2(C15)	1266	νC17-N10	1256	νC18-C20	1264	νC17-N10
	1243 (38)	1238	νC17-N10 ρCH_2(C15)	1257	νC17-N10 ρCH_2(C15)	1239	ρCH_2(C15)	1253	ρCH_2(C15)	1229	νC17-N10 ρCH_2(C15)	1232	ρCH_2(C15)
	1234 (61)	1215	δC15O6H31	1223	δC15O6H31	1201	ρCH_2(C13)	1203	ρCH_2(C13)	1224	δC15O6H31	1210	δC15O6H31

1197	1199 (63)	1191	ρCH$_2$(C13)	1189	ρCH$_2$(C13)	1190	δC12O5H29	1186	δC12O5H29	1184	ρCH$_2$(C13)	1186	ρCH$_2$(C13)
1173	1174 (14)	1161	δC12O5H29	1171	δC12O5H29	1157	δC15O6H31	1168	δC15O6H31	1166	δC12O5H29	1173	δC12O5H29
		1137	νC19-N10	1162	νC19-N10	1144	νC19-N10	1156	νC19-N10	1137	νC19-N10	1162	νC19-N10
1122	1125 (13)	1116	ν_aCF$_3$	1146	νC11-O4	1130	νN9-C11	1111	νN9-C11	1123	ν_aCF$_3$	1116	νN9-C11
	1102 (8)	1110	ν_aCF$_3$ρCF$_3$	1090	νN9-C11	1118	ν_aCF$_3$	1082	νC14-C15	1115	ν_aCF$_3$ρ'CF$_3$	1099	νC11-O4
1096		1097	νN9-C11	1074	ν_aCF$_3$	1100	ν_aCF$_3$	1078	ν_aCF$_3$	1097	νN9-C11	1088	δ_sCF$_3$
1069	1067 (20)	1086	ν_aCF$_3$	1073	ν_aCF$_3$ρ'CF$_3$	1087	νC15-O6	1073	γC18-C20	1095	ν_aCF$_3$	1073	ν_aCF$_3$
1052 sh	1052 (6)	1074	νC15-O6	1061	νC12-O5	1074	δ_aCF$_3$	1056	νC11-O4	1079	νC11-O4	1061	ν_sCF$_3$
		1053	τR$_1$(A5)	1044	νC15-O6	1052	νC14-O4	1038	νC12-C14	1050	νC15-O6	1052	νC14-C15
1026	1029 (10)	1030	νC12-C13	1028	νC12-C13	1039	νC11-C13	1034	δC12C14C15 δO5C12C13	1037	δO4C14C15 νC14-C15	1037	νC15-O6
1012	1016 (26)	1024	γC16-H28	1010	ν_sCF$_3$	1006	γC16-H28	1011	ν_sCF$_3$	1014	νC12-C13	1008	νC12-C13
1000	1003 (7)	1002	τCH$_2$(C15) νC12-O5	989	τCH$_2$(C15)	985	δ_sCF$_3$$\delta_aCF_3$	996	γC16-H28 ν_sCF$_3$	998	γC16-H28	992	δ_sCF$_3$ δ_aCF$_3$
971	974 (5)	991	νC18-C19 ν_sCF$_3$	987	γC16-H28	973	νC11-O4	968	τCH$_2$(C15)	976	γC16-H28	955	γC16-H28
	961 (3)	985	νC14-C15	986	νC14-C15	968	νC12-O5	962	νC15-O6	963	τR$_1$(A5)	951	γC16-H28
957		941	νC12-C14	946	νC12-C14	933	νC11-C13	930	νC11-C13	939	τCH$_2$(C15) νC12-O5	937	τCH$_2$(C15) νC14-O4
903	906 (17)	925	νC11-C13 τCH$_2$(C13)	927	νC11-C13 δO4C11N9	896	νC12-C13 νC12-C13	888	νC12-O5	920	νC11-C13	923	νC11-C13
896 sh	898 (40)	862	δN9C11C13	862	δN9C11C13	859	δO5C12C14	857	δO5C12C14	874	δN9C11C13	877	νC12-O5
882		829	νC14-O4	820	νC14-O4	850	τCH$_2$(C15)	834	νC14-O4	846	βR$_2$(A5)	843	βR$_2$(A5)
870	872 (5)	803	βR$_2$(A5)	814	βR$_2$(A5)	829	τCH$_2$(C13)	819	βR$_2$(A5) τCH$_2$(C13)	792	νC14-O4 νC12-C14 τCH$_2$(C13)	794	νC12-C14 τCH$_2$(C13)
851	853 (38)	764	βR$_1$(A6) νN9-C17	770	βR$_1$(A6)	765	βR$_1$(A6) νN9-C17	767	βR$_1$(A6) νN9-C17	765	βR$_1$(A6)	771	νC18-C19 νN9-C17
793	795 (22)	760	τR$_1$(A6) γC19=O8	759	γC19=O8	760	γC19=O8	758	γC19=O8	760	τR$_1$(A6) γC19=O8	758	γC19=O8 γC18-C20
	772 (29)	750	γC17=O7	748	βR$_1$(A5)	754	βR$_1$(A5) νC11-C13	756	τR$_2$(A6) τR$_1$(A6)	749	γC17=O7	738	γC17=O7
734	737 (31)	745	βR$_1$(A5)	742	τR$_1$(A6) γC17=O7	745	γC17=O7	735	τR$_1$(A6) γC17=O7	733	τR$_2$(A5)	728	νC12-C14
		717	βN9-C11	714	βN9-C11	695	βN9-C11	696	βN9-C11	700	βN9-C11	701	βR$_1$(A5)
	675 (29)	687	γN10-H30	671	γN10-H30	679	τR$_1$(A6)	667	γN10-H30	685	γN10-H30	662	βC17=O7
663		653	βC17=O7 βC19=O8	659	βC17=O7 βC19=O8	661	βC17=O7 βC19=O8	665	βC17=O7 βC19=O8	655	βC17=O7 βC19=O8	650	γN10-H30
632 (7)	623	δO4C11N9 βR$_2$(A6)		624	βR$_2$(A6)	623	βR$_2$(A6) δC14C15O6	626	βR$_2$(A6)	613	δO4C11N9 βR$_2$(A6) βR$_3$(A6)	614	βR$_3$(A6) βR$_2$(A6)
565 (21)	564	βR$_3$(A6)		565	βR$_3$(A6)	597	βR$_1$(A5)	600	βR$_1$(A5) βR$_3$(A6) δC14C15O6	578	γN9-C11 δN9C11C13	562	δO4C11N9
	543	δO4C14-C15		546	δO4C14-C15 δO5C12C14	548	βR$_3$(A6) δO4C11N9	554	δN9C11C13 βR$_3$(A6)	548	δC12C14C15 δO5C12C14δ C14C15O6	553	δC12C14C15 δO5C12C14
	516	δC14C15O6		520	δC14C15O6	523	δ_sCF$_3$$\nu_sCF_3$	537	γN9-C11	525	ν_sCF$_3$	524	δ_sCF$_3$$\nu_sCF_3$
495 (35)	494	γC18-C20		494	γC18-C20	485	ρ'CF$_3$	507	γN9-C11	497	γC18-C20	487	ρ'CF$_3$
474 (6)	458	τR$_3$(A6)		461	τR$_3$(A6)	464	γC18-C20 δN9C11C13	471	δ_aCF$_3$ τR$_3$(A6)	474	τR$_3$(A6)	472	δ_aCF$_3$$\delta_sCF_3$
446 (3)	441	δC12C14C15		446	νN9-C11 δ_sCF$_3$	434	δ_sCF$_3$	432	δ_sCF$_3$	441	τR$_3$(A6)	449	δO5C12C13
421 (7)	423	δO5C12C13		427	τR$_3$(A6)	417	δO5C12C13	423	γN9-C11	423	γN9-C11	423	δ_sCF$_3$
397 (16)	407	δ_sCF$_3$		407	δO5C12C13	392	δ_sCF$_3$	394	δ_sCF$_3$	407	τR$_3$(A6) τR$_1$(A6)	404	τR$_3$(A6) τR$_1$(A6)

378 (28)	384	τR_3(A6)	382	τR_3(A6) τR_1(A6)	371	$\delta_s CF_3$	381	γC18-C20	383	$\delta_s CF_3$	391	$\delta_s CF_3$
342 (3)	348	$\delta_s CF_3$	350	γN9-C11	355	$\delta_s CF_3$	346	$\delta_s CF_3$	346	γN9-C11	358	$\delta_s CF_3$
304 (21)	339	τR_2(A5) δO5C12C14	340	τR_1(A6)	340	δO4C14-C15	338	δO4C14-C15	310	$\delta_s CF_3$	314	$\delta_s CF_3$
	328	$\delta_s CF_3$	325	βN9-C11 $\delta_s CF_3$	315	$\delta_s CF_3$	300	$\delta_s CF_3$	300	τO5-H29	304	$\delta_s CF_3$
298 (24)	293	$\rho CF_3 \tau$O5-H29	295	ρCF_3	295	$\delta_s CF_3$	297	τO5-H29	280	ρCF_3	290	$\delta_s CF_3 \delta_s CF_3$
276 (9)	276	$\delta_s CF_3$	265	τO5-H29	291	τO5-H29	267	τO6-H31	254	τO6-H31	269	τO5-H29
	256	γN9-C11	255	$\delta_s CF_3$	270	$\delta_s CF_3$	234	τR_2(A5)	244	γN9-C11	263	$\delta_s CF_3$
				γN9-C11		$\delta_s CF_3$				$\delta_a CF_3$		$\delta_s CF_3$
	249	τO6-H31	244	$\delta_a CF_3 \delta_s CF_3$	251	τO6-H31	226	$\delta_a CF_3$	231	$\delta_a CF_3 \delta_s CF_3$	243	δC14C15O6
	225	$\delta_s CF_3$	214	τwC11-N9	239	$\delta_a CF_3$	207	$\delta_s CF_3 \delta_s CF_3$	204	$\delta_a CF_3 \delta_s CF_3$	215	βN9-C11
180 sh	199	$\delta_a CF_3 \delta_s CF_3$	185	δC12C14C15 τO6-H31	222	δC12C14C15	161	$\delta_s CF_3 \delta_a CF_3$	171	γN9-C11	176	ρCF_3
175 sh	170	$\delta_a CF_3 \delta_s CF_3$	170	$\delta_s CF_3 \tau R_1$(A6)	168	ρCF_3	155	τR_2(A6)	160	τR_2(A6)	165	τO6-H31
	161	τR_2(A6)	166	τR_2(A6)	155	γN10-H30	155	$\delta_a CF_3 \delta_s CF_3$	157	$\delta_a CF_3 \delta_s CF_3$	156	τR_1(A6) γN10-H30
	149	τR_2(A6)	152	τR_2(A5)	154	τR_3(A6)	121	τwC15-O6	144	τR_2(A6) $\delta_a CF_3 \delta_s CF_3$	143	τR_2(A6)
120 (35)	137	τwC15-O6	146	τwC15-O6	130	τwC15-O6	112	$\delta_s CF_3$	128	τwC11-N9	135	δO4C14-C15
100 (9)	102	τR_1(A5)	110	τR_1(A5)	108	βC18-C20	99	$\delta_s CF_3$	104	$\delta_s CF_3$	116	τR_1(A5)
	90	$\delta_s CF_3$	91	$\delta_s CF_3$	104	τR_1(A5)	93	τR_1(A5)	89	τwC15-O6	94	τwC15-O6
78 (35)	83	τwC11-N9	79	τwC11-N9	71	γN9-C11	75	τwC11-N9	78	$\delta_s CF_3$	75	γN9-C11
70 sh	63	$\delta_s CF_3 \tau$w CF_3	57	τw CF_3	57	γN10-H30	49	τw CF_3	59	τw CF_3	56	τR_3(A6)
60 (3)	34	τw CF_3	48	$\delta_s CF_3$	46	τR_2(A5)	40	$\delta_s CF_3$	29	$\delta_a CF_3 \tau$w CF_3	39	τR_2(A5)
50 sh	28	$\delta_s CF_3$	29	$\delta_s CF_3$	29	τwC11-N9	30	$\delta_s CF_3$	25	$\delta_s CF_3$	34	τw CF_3
	22	$\delta_s CF_3$	22	$\delta_s CF_3$	22	τw CF_3	24	$\delta_s CF_3$	15	$\delta_s CF_3$	25	τwC11-N9

ν, stretching; δ, scissoring; wag, wagging or out- of plane deformation; ρ, rocking; τ, torsion; twist, twisting; a, antisymmetric; s, symmetric ; ip, in-phase; op, out-of-phase; R, ring; pyrimidine ring,(A6); sugar ring, (A5)

[a]This work, [b]From Ref [32], [c]From Ref [42], [d]From scaled quantum mechanics force field B3LYP/6-31G*

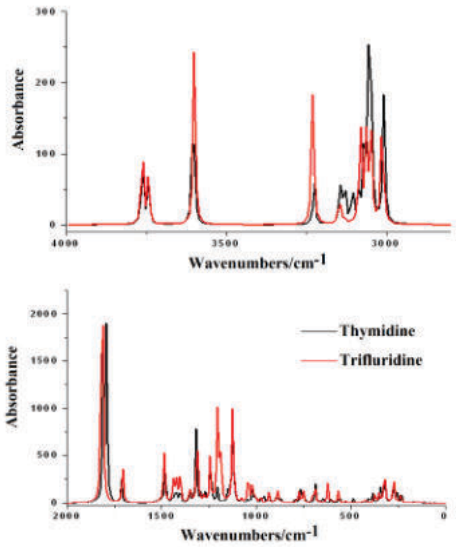

Figure 13. Comparisons between the theoretical infrared spectra of the C3 conformer of thymidine with the corresponding to the C3 isomer of trifluridine at B3LYP/6-31G* level of calculation.

In thymidine, the NH out-of-plane deformation modes are assigned to the IR band at 663 cm^{-1}, here these modes are predicted between 668 and 650 cm^{-1} and also, coupled with other modes at lower wavenumbers.

Cf_3 modes. The antisymmetric and symmetric CF_3 stretching modes corresponding to the C1, C3 and C5 isomers of TFT are predicted between 1123 and 996 cm^{-1} while the corresponding antisymmetric and symmetric deformation modes are strongly coupled with a great quantity of modes in the lower wavenumbers region, as can be seen in Table 14. Hence, the rocking modes in the three isomers are predicted overlapped with these deformation modes. The twisting modes corresponding to these groups are predicted by calculation between 63 and 34 cm^{-1}, as indicated in Table 14.

Ch_2 modes. In thymidine, the CH_2 stretching modes are predicted between 3034 and 2851 cm^{-1} while in the isomers of TFT between 3035 and 2868 cm^{-1}, hence they can be assigned in the same region. Obviously, these modes are not affected by the introduction of the CF_3 groups. The scissoring modes are predicted by the calculations between 1492 and 1427 cm^{-1} while the wagging modes between 1485 and 1327 cm^{-1}. Also, some of these modes are predicted coupled with the rocking modes. The SQM calculations predicted the rocking modes for the three isomers between 1327 and 1197 cm^{-1} while in thymidine those modes are predicted between 1288 and 1173 cm^{-1}. Finally, the twisting modes in the three isomers are predicted in different regions, in some isomers coupled with other modes, thus, in C1, C3 and C5 these modes are predicted in the 1002-995, 968-819 and 939-792 cm^{-1} regions, respectively.

Skeletal modes. In the three isomers of TFT, the C=O and C=C stretching modes are predicted in the same regions that in three conformers of thymidine [32], for these reasons, they can be easily assigned in these regions. The N9-C16 stretching modes in the three isomers are predicted by SQM calculations at higher wavenumbers (1458-1439 cm^{-1}) and, for this reason, they have a partial double bond character while the C17-N10 are calculated between 1266 and 1256 cm^{-1}, as observed in Table 14. The remains N9-C11 and N9-C17 stretching modes are observed at

lower wavenumbers, as expected because the corresponding bonds have simple bond characters. Finally, in Table 14 are identified and assigned the remaining vibration modes.

FORCE FIELD

Here, the Molvib program [24] and the SQM procedure were used to compute the force fields of the three isomers of TFT in gas and aqueous solution phases, later, with these scaled force fields, the force constants expressed in valence internal coordinates were computed. The results can be seen in **Table 15** compared with the values obtained for thymidine and zalcitabine because both antiviral agents are pyrimidine analogues [32,42]. First, when the values for the three isomers are compared among them we observed in general that the lower values are computed in solution.

TABLE – 15 Scaled force constants for the most stable isomers of trifluridine in gas and aqueous solution phases

	B3LYP/6-31G*										
	Trifluridine[a]					Thymidine[b]		Zalcitabine[c]			
Force constant	Gas	Gas	PCM	Gas	PCM	Gas	PCM	Gas		PCM	
	C1	C3	C3	C5	C5	C3	C3	C1	C2	C1	C2
f(νO-H)	7.25	7.23	7.15	7.25	7.19	7.25	7.17	7.15	7.17	7.14	7.19
f(νN-H)	6.60	6.61	6.50	6.60	6.45	6.62	6.49	6.79	6.82	6.78	6.74
$f(\nu C\text{-}H)_{A6}$	5.20	5.25	5.10	5.40	5.39	5.22	5.25	5.30	3.48	5.38	5.31
$f(\nu C\text{-}H)_{A5}$	4.60	4.83	4.87	4.80	4.87	4.83	5.08	4.80	4.65	4.84	4.74
f(νC=C)	11.50	8.09	11.50	11.70	7.90	8.17	8.09	7.83	7.97	7.92	8.07
f(νC=O)	11.85	11.89	10.80	11.85	10.83	11.63	10.50	11.30	11.45	9.72	9.99
$f(\nu C\text{-}O)_{A5}$	5.15	4.52	4.45	4.80	4.59	4.48	4.26	4.36	4.47	4.68	4.27
$f(\nu C\text{-}O)_{OH}$	5.10	4.90	4.75	5.05	4.82	4.88	4.74	5.18	5.09	4.83	4.79
f(νC-N)	6.28	5.39	6.32	6.30	5.46	5.38	5.45	5.99	6.01	6.06	6.09
$f(\nu C\text{-}C)_{A6}$	5.20	4.83	5.50	5.20	5.08	4.88	5.12	5.57	5.55	5.73	5.73
$f(\nu C\text{-}C)_{A5}$	3.97	3.89	4.07	4.03	3.96	3.86	3.91	3.96	3.96	3.98	3.97
f(H-C-H)	0.80	0.77	0.75	0.75	0.76	0.77	0.76	0.76	0.54	0.74	0.74
f(C -O-H)	0.70	0.70	0.70	0.70	0.72	0.70	0.73	0.83	0.82	0.79	0.75

ν, stretching; δ, angle deformation. Units in mdyn $Å^{-1}$ for stretching and mdyn Å rad^{-2} for angle deformations

[a]This work, [b]From Ref [32], [b]From Ref [43]

TABLE – 16 TD-DFT calculated visible absorption wavelengths (nm) for the C1, C3 and C5 isomers of trifluridine in aqueous solution

Experimental				B3LYP method[a]			
Thymidine[b]	Idoxuridine[c]			Trifluridine			Assignment[a]
Water[b]	Methanol[c]	Water[c,d]	0.1M	C1	C3	C5	
				136 vs			$\pi^* \rightarrow \pi^*$ *C=O*
				155 sh	157 sh	151 sh	$n \rightarrow \sigma^*$ *F1, F2, F3, O4, O7, O8*
				174 s	174 vs	165 vs	$\pi \rightarrow \pi^*$ *C=C*
211	227	217	217	220 m	220 m	212 m	$\pi \rightarrow \pi^*$ *C=O*
268	284	288	288	290 w	290 w	269 w	$n \rightarrow \pi^*$ *N9, N10*

[a]This work, [b]Ref. [44], [c]Ref. [45], [d]Ref. [46]

Thus, the decreasing of the force constants especially, the *f(O-H), f(νN-H), f(νC=O)* and *f(νC-O)* force constants can be attributed to the H bonds formation of these groups with water molecules. Comparing the values of C3 of TFT with C3 of thymidine, we observed that the *f(O-H)* and *f(νN-H)* force constants remain practically constant, as expected because the vibrational analysis reveal that the positions of these stretching modes not change when the CH_3 group is replaced by the CF_3 group. The higher changes are observed in the *f(νC-N), f(νC-C)*$_{A6}$ and *f(νC-C)*$_{A5}$ force constants because, for example, the charges and bond orders of the involved atoms change in those two species, as observed in the above studies. When the values are compared with those obtained for the C1 and C2 conformers of zalcitabine, the *f(O-H)* force constants of these species have lower values than TFT because both conformers of this species have one OH group while the higher values of the *f(νN-H)* force constants in zalcitabine are justified because it antiviral agent has one NH_2 group instead a NH group as in the isomers of TFT. In the three antiviral agents are observed the reduction of their values in solution as a consequence of the hydration of the involved groups in the H bond formation.

ELECTRONIC SPECTRUM

The predicted UV-visible spectra for the three isomers of TFT in aqueous solution at the B3LYP/6-31G* level of theory are compared with the available experimental spectra for thymidine in aqueous solution taken from Ref [44] in **Figure 14**. **Table 16** shows the TD-DFT calculated visible absorption wavelengths for the C1, C3 and C5 isomers of trifluridine in aqueous solution where clearly are indicated the positions and intensities of the bands. Besides, the available experimental bands observed for idoxuridine in methanol, water and 0.1 M HCl solutions [45,46] were also included to comparison. The charge transfers observed in the NBO analysis were used to assign the main bands, thus, the very intense bands are assigned to the $\pi^* \rightarrow \pi^*$ transitions attributed to the C=O and C=C bonds of both species while the remain bands can be assigned to the $n \rightarrow \sigma^*$ and $n \rightarrow \pi^*$ transitions due to the lone pairs of the F, N and O atoms. Here, the intensity of the most intense band observed for thymidine probably can justify the higher ΔE_{Total} observed for thymidine than TFT. This way, this result could in part explain the different biological properties observed for thymidine than TFT.

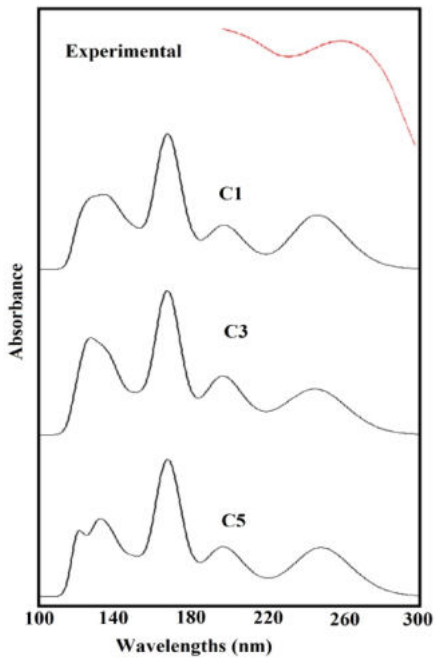

Figure 14. Comparisons between the experimental electronic spectra of thymidine with the corresponding to the C1, C3 and C5 isomers of trifluridine in aqueous solution at B3LYP/6-31G* level of calculation.

CONCLUSIONS

In the present work, the molecular structures of five stable isomers of trifluridine have been studied by using the hybrid B3LYP/6-31G* method in gas and aqueous solution phases. These most stable structures are in very good agreement with that experimental determined by X-ray diffraction. The structural and vibrational properties of those three most stable isomers with higher populations were determined using NBO, MEP, QAIM and SQMFF calculations. The results for those three isomers were compared with the most stable conformer of thymidine in order to observe the differences in the properties when the CF_3 group is replaced by a CH_3 group. Thus, we observed that both *Cis* conformations are the most stable than the other ones while the presence of the F atoms in the structure of TFT increase the volume, as compared with thymidine. Probably, the proximities between the O4 and O6 atoms in TFT increase the instability of these structures, in relation to thymidine. The charges on the C atoms attached to the F atoms in TFT are higher and positive in reference to thymidine and as a consequence the MEP value in thymidine and their bond orders are highest in this species than TFT. The NBO calculations reveal a higher stability for thymidine than TFT while the QAIM studies support the high stabilities of the *Cis* isomers in both antiviral agents. The study of the frontier orbitals evidence that the CF_3 group in the pyrimidine rings increase the gap values diminishing their reactivities while the iodine atom in the pyrimidine ring of idoxuridine decrease the gap value and, as a consequence increase their reactivity. The descriptors show that the incorporation of a CF_3 group or of an iodine atom in the pyrimidine rings increases the electrophilicity and nucleophilicity indexes in TFT and idoxuridine, as compared with thymidine.

The vibrational study support the differences between TFT and thymidine due to the exchange of CF_3 by CH_3 while the OH stretching modes are more affected by the CF_3 groups than the corresponding deformation modes. The complete assignments of the three isomers of TFT, the force fields and the force constants of stretching and deformations are presented for those three isomers of TFT. The comparisons of the theoretical IR, ^{1}H-NMR, ^{13}C-NMR and UV-visible spectra with the corresponding to thymidine show clearly the differences with this species due to the CH_3 group, as it is expected.

ACKNOWLEDGEMENTS

This work was supported with grants from CIUNT Project Nş 26/D207 (Consejo de Investigaciones, Universidad Nacional de Tucumán). The authors would like to thank Prof. Tom Sundius for his permission to use MOLVIB.

REFERENCES:

[1] De Clercq, E. (2004). Antiviral drugs in current clinical use, Journal of Clinical Virology, 30115–30133.
[2] De Clercq, E.; Descamps, J.; De Somer, P.; Barrt, P. J.; Jones, A. S.; Walker, R. T. (1979). (E)-5-(2-Bromovinyl)-2'-deoxyuridine: A potent and selective anti-herpes agent, Proc. Natl. Acad. Sci.76(6), 2947-2951.
[3] De Clercq, E. (2011). Antiviral Drug Strategies, First Edition. Wiley-VCH Verlag GmbH & Co. KGaA. Published 2011 by Wiley-VCH Verlag GmbH & Co. KGaA.
[4] Sanmarti, B.; Berenguer, M.; Maimo, R.; Solsona Rocabert, J.G. (2011) EUROPEAN PATENT APPLICATION, EP 2 377 862 A1 19.10.2011 Bulletin 2011/42.
[5] Hobden, J. A.; Kumar, M.; Kaufman, H. E.; Clement, C.; Varnell, E. D.; Bhattacharjee, P. S.; Hill, J. M. (2011). In Vitro Synergism of Trifluorothymidine and Ganciclovir against HSV-1, IOVS, 52(2), 830-833.
[6] Nukatsuka, M.; Nakagawa, F.; Takechi, T. (2015). Efficacy of Combination Chemotherapy Using a Novel Oral Chemotherapeutic Agent, TAS-102, with Oxaliplatin on Human Colorectal and Gastric Cancer Xenografts, Anticancer Research 35, 4605-4616.
[7] Tanaka, N.; Sakamoto, K.; Okabe, H.; Fujioka, A.; Yamamura, K.; Nakagawa, F.; Nagase, H.; Yokogawa, T.; Oguchi, K.; Ishida, K.; Osada, A.; Kazuno, H.; Yamada, Y.; Matsuo, K. (2014). Repeated oral dosing of TAS-102 confers high trifluridine incorporation into DNA and sustained antitumor activity in mouse models, Oncology Reports 32, 2319-2326.
[8] Azijli, K.; van Roosmalen, I. A. M.; Smit, J.; Yuvaraj, S.; Fukushima, M.; de Jong, S.; Peters, G. J.; Bijnsdorp, I. V. A.; Kruyt, E F. (2014). The novel thymidilate synthase inhibitor trifluorothymidine (TFT) and trail synergistically erradícate non-small cell lung cancer cells, Cancer Chemotherapy and Pharmacology; 73(6), 1273-1283
[9] Bijnsdorp, I. V.; Temmink, O. H.; Prins, H-J.; Losekoot, N.; Adema, A. D.; Smid, K.; Honeywell, R. J.; Ylstra, B.; Eijk, P. P.; Fukushima, M.; Peters, G. J. (2010). Trifluorothymidine resistance is associated with decreased thymidine kinase and equilibrative nucleoside transporter expression or increased secretory phospholipase A2, Molecular Cancer Therapeutics 9, 1047-1057.
[10] Langen P.; Kowolljk, G. (1968). 5'-Deoxy-5'-Fluoro-Thymidine, a Biochemical Analogue of Thymidine- 5'-Monophosphate Selectively Inhibiting DNA Synthesis, European J. Biochem. 6, 344-351.
[11] Hajjawi, O. S. (2015). Ribonucleic acid (RNA) biosynthesis in human cancer, Cancer Cell International 15(22), 1-14.
[12] Fresco-Taboada, A.; Serra, I.; Fernández-Lucas, J.; Acebal, C.; Arroyo, M.; Terreni, M.; de la Mata, I. (2014). Nucleoside 2'-Deoxyribosyltransferase from Psychrophilic Bacterium Bacillus psychrosaccharolyticus- Preparation of an Immobilized Biocatalyst for the Enzymatic Synthesis of Therapeutic Nucleosides, Molecules, 19, 11231-11249.
[13] Low, J. N.; Tollin, P.; Howie, R. A. (1989). Structure of 5-(trifluoromethyl)-2'-deoxyuridine, Acta Cryst. C45, 99-101.
[14] Sultana, T.; Khan, Md. W. (2013). A Facile Synthesis of 5-Iodo-6-Substituted Pyrimidines from Uracil-6-Carboxylic acid (Orotic acid), Dhaka Univ. J. Pharm. Sci.12(2), 97-102.
[15] Çırak, Ç.; Koç, N. (2012). Molecular structure and effects of intermolecular hydrogen bonding on the vibrational spectrum of trifluorothymine, an antitumor and antiviral agent J. Mol. Model. 18, 4453–4464.
[16] Puffer, B.; Kreutz, C.; Rieder, U.; Ebert, M-O.; Konrat, R.; Micura, R. (2009). 5-Fluoro pyrimidines: labels to probe DNA and RNA secondary structures by 1D 19F NMR spectroscopy, Nucleic Acids Research, 37(22), 7728–7740.
[17] Becke, A.D. (1993). Density functional thermochemistry. III. The role of exact exchange J. Chem. Phys. 98, 5648-5652.
[18] Lee, C.; Yang, W.; Parr. R.G. (1988), Development of the Colle-Salvetti correlationenergy formula into a functional of the electron density, Phys. Rev. B37, 785-789.
[19] Tomasi, J.; Persico, J. (1994), Molecular Interactions in Solution: An Overview of Methods Based on Continous Distributions of the Solvent, Chem. Rev. 94, 2027-2094.
[20] Miertus, S.; Scrocco, E.; Tomasi, J. (1981), Electrostatic interaction of a solute with a continuum. Chem. Phys. 55, 117–129.
[21] Marenich, A.V.; Cramer, C.J.; Truhlar, D.G. Universal solvation model based on solute electron density and a continuum model of the solvent defined by the bulk dielectric constant and atomic surface tensions, J. Phys. Chem. B113 (2009) 6378-6396.
[22] Ugliengo, P. Moldraw Program, University of Torino, Dipartimento Chimica IFM, Torino, Italy (1998).
[23] a) Rauhut, G.; Pulay, P. (1995), J. Phys. Chem. 99 (1995) 3093-3099. b) Correction: G. Rauhut, P. Pulay, J. Phys. Chem. 99, 14572.
[24] Sundius, T. (2002), Scaling of ab initio force fields by MOLVIB, Vib. Spectrosc. 29, 89-95.
[25] Nielsen, A.B.; Holder A.J. Gauss View 5.0, User's Reference, GAUSSIAN Inc., Pittsburgh, PA (2008).
[26] Gaussian 09, Revision D.01, Frisch, M. J.; Trucks, G. W.; Schlegel, H. B.; Scuseria, G. E.; Robb, M. A.; Cheeseman, J. R.; Scalmani, G.; Barone, V.; Mennucci, B.; Petersson, G. A.; Nakatsuji, H.; Caricato, M.; Li, X.; Hratchian, H. P.; Izmaylov, A. F.; Bloino, J.; Zheng, G.; Sonnenberg, J. L.; Hada, M.; Ehara, M.; Toyota, K.; Fukuda, R.; Hasegawa, J.; Ishida, M.; Nakajima, T.; Honda, Y.; Kitao, O.; Nakai, H.; Vreven, T.; Montgomery, J. A., Jr.; Peralta, J. E.; Ogliaro, F.; Bearpark, M.; Heyd, J. J.; Brothers, E.; Kudin, K. N.; Staroverov, V. N.; Kobayashi, R.; Normand, J.; Raghavachari, K.; Rendell, A.; Burant, J. C.; Iyengar, S. S.; Tomasi, J.; Cossi, M.; Rega, N.; Millam, J. M.; Klene, M.; Knox, J. E.; Cross, J. B.; Bakken, V.; Adamo, C.; Jaramillo, J.; Gomperts, R.; Stratmann, R. E.; Yazyev, O.; Austin, A. J.; Cammi, R.; Pomelli, C.; Ochterski, J. W.; Martin, R. L.; Morokuma, K.; Zakrzewski, V. G.; Voth, G. A.; Salvador, P.; Dannenberg, J. J.; Dapprich, S.; Daniels, A. D.; Farkas, Ö.; Foresman, J. B.; Ortiz, J. V.; Cioslowski, J.; Fox, D. J. Gaussian, Inc., Wallingford CT, 2009.
[27] Glendening, E.D.; Badenhoop, J.K.; Reed, A.D.; Carpenter, J.E.; Weinhold, F. NBO 3.1; Theoretical Chemistry Institute, University of Wisconsin; Madison, WI, 1996.
[28] Biegler-Köning, F.; Schönbohm, J.; Bayles, D. (2001), AIM2000; A Program to Analyze and Visualize Atoms in Molecules, J. Comput. Chem. 22, 545.
[29] Parr, R.G.; Pearson, R.G. (1983), Absolute hardness: companion parameter to

absolute electronegativity, J. Am. Chem. Soc. 105, 7512-7516.
[30] Brédas, J-L (2014), Mind the gap!, Materials Horizons 1, 17-19.
[31] Cataldo, P.G.; Castillo, M.V.; Brandán, S.A. (2014), Quantum Mechanical Modeling of Fluoromethylated-pyrrol Derivatives a Study on their Reactivities, Structures and Vibrational Properties, J Phys Chem Biophys, 4(1), 4-9.
[32] Márquez, M. B.; Brandán, S. A. (2014). A structural and vibrational investigation on the antiviral deoxyribonucleoside thymidine agent in gas and aqueous solution phases. 0020-7608. International J. of Quantum Chem. 114(3), 209-221.
[33] Márquez, M.J.; Márquez, M.B.; Cataldo, P.G.; Brandán, S.A. (2015). A Comparative Study on the Structural and Vibrational Properties of Two Potential Antimicrobial and Anticancer Cyanopyridine Derivatives, A Open Journal of Synthesis Theory and Applications, 4, 1-19.
[34] Romani, D.; Márquez, M.J.; Márquez, M.B.; Brandán, S.A. (2015). Structural, topological and vibrational properties of an isothiazole derivatives series with antiviral activities, J. Mol. Struct. 1100 279-289.
[35] Romani, D.; Brandán, S.A. (2015), Structural, electronic and vibrational studies of two 1,3-benzothiazole tautomers with potential antimicrobial activity in aqueous and organic solvents. Prediction of their reactivities, Computational and Theoretical Chem., 1061, 89-99.
[36] Romani, D.; Brandán, S.A. (2015), Effect of the side chain on the properties from cidofovir to brincidofovir, an experimental antiviral drug against to Ebola virus disease, Arabian Journal of Chemistry
http://dx.doi.org/10.1016/j.arabjc.2015.06.030.
[37] Ditchfield, R. (1974). Self-consistent perturbation theory of diamagnetism. I. A gageinvariant LCAO (linear combination of atomic orbitals) method for NMR chemical shifts, Mol. Phys. 27, 714e722.
[38] Besler, B.H.; Merz Jr., K.M.; Kollman, P.A. (1990).Atomic charges derived from semiempirical methods, J. Comp. Chem. 11, 431e439.
[39] Bushmarinov, I.S.; Lyssenko, K.A.; Antipin, M.Y. (2009). Atomic energy in the Atoms in Molecules theory and its use for solving chemical problems, Russian Chem. Rev. 78(4), 283-302.
[40] Available from: http://www.sigmaaldrich.com/spectra/fnmr/FNMR006943.PDF
[41] Available from: http://www.chemicalbook.com/SpectrumEN_50-89-5_1HNMR.htm
[42] Tsuboi, M., Komatsu, M., Hoshi, J., Kawashima, E., Sekine, T., Ishido, Y., Russell, M. P., Benevides, J. M.; Thomas, G. J. Jr, (1997). Raman and Infrared Spectra of (2'S)-[2'-2H]Thymidine: Vibrational Coupling between Deoxyribosyl and Thymine Moieties and Structural Implications, J. Am. Chem. Soc., 119, 2025-2032.
[43] Checa, M.A., Rudyk, R., Chamorro, E.E., Brandán, S.A. (2014). Structural Properties of a Reverse Inhibitor against the HIV Virus, Dideoxynucleoside Zalcitabine in Gas and Aqueous Solution Phases, QUITEL, Gapalago's Island, Ecuador.
[44] Available from: http://webbook.nist.gov/cgi/cbook.cgi?ID=C50895&Mask=400#UV-Vis-Spec
[45] Available from: https://www.pmda.go.jp/files/000152703.pdf
[46] Available from: http://newdrugapprovals.org/2014/08/31/idoxuridine/*, ETn * and ETn *